UNIVERSITY OF CALIFORNIA

RIVERSIDE

Investigating the Relationship Between Sapwood Density and Sapwood Capacitance Within the Hydraulic Pipeline Paradigm

A Thesis submitted in partial satisfaction
of the requirements for the degree of

Master of Science

in

Evolution, Ecology, and Organismal Biology

by

Erika Rose Bucior

June 2020

Thesis Committee:

Dr. Louis Santiago, Chairperson

Dr. Helen Regan

Dr. Marko Spasojevic

The Thesis of Erika Rose Bucior is approved:

_____

_____

_____

Committee Chairperson

ACKNOWLEDGEMENTS

I would like to first acknowledge and thank Jason Hamilton, who encouraged me to sit in the woods once a week and key out as many trees as possible during my first semester as an undergraduate. After that, Peter Melcher became my mentor for four years. His tough love and passion for teaching afforded me numerous experiences and opportunities to fully pursue this new passion and grow in ways that would benefit what I hope to be a long career in ecophysiology.

I would like to thank my current advisor and mentor Lou Santiago, who has also continuously supported my work and helped me grow and develop the skills needed for me to grow into the person and scholar that I had hoped to be. I have received a lot of help and encouragement from past and current members of the Santiago lab including: Alexandria Pivovaroff, Eleinis Avila-Lovera, Aleyda Acosta Rangel, Jose-Luiz Silva, Ariana Firebaugh-Ornelas, Denise Mitchel, and Eric Ngo. My guidance and thesis committee members Helen Regan and Marko Spasojevic have also provided me with invaluable feedback and guidance during my three years at UC Riverside.

The fearless Edwin Andrade always kept me safe and smiling during my fieldwork at the Smithsonian Tropical Research Institute and I couldn't have done any of the work without the help of my dear friends and fellow researchers Anna Shats and Charlotte Steeves. Joe Wright and Martijn Slot also provided me with essential technical assistance when our equipment was misbehaving.

Funding for my work in Panama was provided by the Centre for the Study of Amazonian Biodiversity (CEBA) and the Smithsonian Tropical Research Institute. Funding for fieldwork in California was provided by the UC Riverside EDGE institute and the UC Natural Reserve System's Institute for the Study of Ecological and Evolutionary Climate Impacts (ISEECI).

The fact that I have had any of these opportunities is entirely due to the extreme selflessness and constant love from my parents. They may not always exactly understand what I do, but they continue to make every sacrifice needed for me to pursue my passions. I convinced my sister to join a plant biology lab alongside me her second year at Ithaca. Although she didn't end up falling in love with the same specialty, her understanding of my ambitions and watching me in my element has allowed her to always understand how I'm feeling during stressful times.

And to end on a lighter note, my college friends, aka "Squad", were instrumental in maintaining my mental and emotional health. I thank them for the countless nights of dance parties over skype, visits, and all the supportive late-night chats spanning five different time zones.

To the memory of my grandparents Anastasia and Peter Bucior

ABSTRACT OF THE THESIS

Investigating the Relationship Between Sapwood Density and Sapwood Capacitance Within the Hydraulic Pipeline Paradigm

by

Erika Rose Bucior

Master of Science, Graduate Program in Evolution, Ecology and Organismal Biology
University of California, Riverside, June 2020
Dr. Louis Santiago, Chairperson

As the earth's climate continues to change, forests within a diverse set of biomes are experiencing increasingly frequent, severe, and longer periods of drought stress. The continued rise of global temperatures could radically alter the composition and structure of forests in many regions (Van Mantgem, 2007). As local and global climate continues to change and drought recurrence increases, understanding subsequent changes within and between these systems is crucial for evaluating how ecosystem services and dynamics will be altered.

Plant hydraulics bridges physiological regulation of transpiration to the environmental drivers of climate. However, the current parameters used to model plant drought responses are unresolved (Sperry, 2015). Previous studies have parameterized tree mortality associated with drought using the value of water potential where 50% of water transport capacity is lost (P50). However, observations of tree mortality combined with direct measurements of P50 are weakly correlated, revealing a critical

inconsistency in what physiologists believe to be the main mechanism in plant-water regulation under stress (Breshears, 2009). Based on accumulating evidence that functional tradeoffs play a significant role in hydraulic performance, we hypothesize that water movement in sapwood, described in terms of sapwood capacitance, is an important component of maintaining hydraulic efficiency under increased water stress.

In this study I determine xylem pressure-volume relationships across a variety of woody plant functional types and across global biome types to increase our understanding of the dynamics of water movement in sapwood. First, I evaluated the relationship between sapwood density and sapwood capacitance. Then I looked at the relationships that these parameters have with other important hydraulic traits at the global and biome level. And finally, I evaluated the role that other morphological or environmental aspects have in influencing these traits and their subsequent sequential tradeoffs.

TABLE OF CONTENTS

LIST OF FIGURES

LIST OF TABLES

Introduction

The continued rise of global temperatures is radically altering the composition and structure of forests in many regions due to increasingly frequent, severe, and longer periods of drought (Van Mantgem et. al 2007). Recent reviews of drought-induced tree mortality have observed that mortality events include cases of large scale die-offs that span broad gradients of ecosystems, from monsoonal savannas to tropical rainforests, and this phenomenon is only expected to increase under many other future climate change scenarios (Allen et. al 2010, Anderegg et al. 2016). Aside from the economic value associated with the ecosystem services provided by such stands of forest and vegetation, the loss of biomass has ramifications that are closely tied to major climate and hydrological feedbacks through loss of stored carbon and altered water cycling (Van Mantgem et. al 2007). Assessing mortality vulnerability across plant functional types and biomes is vital for creating accurate assessments of the effects that climate extremes have on vegetation. However, the physiological traits associated with predicting elevated risk of mortality in diverse ecosystems still remain under debate (Anderegg et al. 2016).

Drought-induced tree mortality has been particularly challenging to model and predict because of the breadth of unresolved compensatory actions that occur within an individual and uncertainty surrounding the final physiological failure underlying tree death (Körner 2019, Anderegg et. al 2016, McCulloh et al. 2019). Despite the multitude of tradeoffs (leaf shedding, deep rooting, biomass allocation shifts, regulation of gas

exchange), the failure of the plant vascular hydraulic transport system is considered the predominant determinant of tree mortality (Santiago et al. 2019, Anderegg et al. 2016). During periods of drought, low soil moisture coupled with high atmospheric evaporative demand cause varying spans of increasingly negative water potentials (Passioura 1982, Venturas et. al 2017). As the water potential decreases, air is aspirated into xylem vessels, expanding to form embolisms and restrict water flow through xylem vessels (Venturas et al. 2017). The way in which each individual species responds to the varying degree of stress is what ultimately determines the extent of the loss of conductivity and hydraulic capability of the tree (Holbrook, 1995, Pivovaroff et al. 2016). Even though individual species have unique configurations of xylem organization to facilitate optimal safety and efficiency, mortality can still occur even if some portion of the xylem is still functional (Hammond, 2019). The point at which a particular species experiences its lethal accumulation of embolism is determined by a unique assemblage of plant hydraulic, stomatal, and allometric traits (Pivovaroff et al. 2016, Santiago et al. 2016, Choat et al. 2018). Identifying the limitations of the compensatory interactions of these traits within diverse plant communities is essential to further untangle the mechanisms which cause mortality.

While the general sequence of hydraulically induced plant mortality is understood (Bartlett et al. 2016), we also know that multiple organ systems play a role in maintaining conductivity and buffering water loss. However, it has been shown extensively that woody dicots display a typical trait sequence and synchrony in hydraulic

compensation in order to limit substantial tissue damage during drought (Bartlett et al. 2016, Manzoni et al. 2014, Mencuccini et al. 2015). As water potentials become increasingly negative, stem conductivity declines, followed by a loss of conductivity in the leaf, leaf wilting, and a progressive loss of conductivity in the stem, resulting in embolism refilling attempts before the plant reaches a lethal threshold of conductivity loss (Bartlett et al. 2016, Meinzer et al. 2013). However, unique assemblages of cell types, varying configurations of cells within tissues and diverse biomass distribution patterns within organs and whole plants raise questions about whether this general sequence represents a universal model of hydraulic failure. Adaptive variations and recombination of such properties play a role in affecting both mechanical and hydraulic performance, suggesting that the aforementioned progression of hydraulic failure may be overlooking novel compensatory traits that have a universal function in all xylem distributions. One potentially important anatomical component that may be overlooked is the role of water storage in sapwood.

Sapwood capacitance, the stored water in stem parenchyma that can temporarily provide water needed to protect xylem from abrupt drops in water potential, has emerged as a key trait for equipping trees to survive drought (Meinzer et al. 2008, Pivovaroff et al. 2016, Pratt et al. 2007, McCulloh et al. 2014). This water is released from either elastic compartments (parenchymatous tissue) or inelastic compartments (apoplastic capillary spaces and vessel lumens) (Holbrook, 1995). Species with higher capacitance may experience fewer embolisms because they are buffered by

stored water which delays critical xylem water potential from being reached and subsequent hydraulic collapse (Santiago et. al 2016, Sperry et. al 2008, Meinzer et al. 2009). This capacitive release of stored water before cavitation provides a short-term buffering effect on water transport (Höltta et al. 2009). The only other mechanisms that can provide additional water recovery/storage are elastic deformation of xylem vessels and capillary storage in wood fibers. (Santiago et al. 2016, Tyree et al. 2002, Perämäki et al. 2001).

The various organizations of cell types in xylem sapwood play individual roles in the transport, storage, and release of water. Differences in wood structure and anatomical variation not only determine and limit the physiological capabilities of hydraulic functioning, they also play an essential role in determining sapwood water storage properties (Holbrook et al. 2011). Early work in this area found that co-occurring species had ranges of capacitance from 83 to 416 kg m^{-3} Mpa^{-1} when capacitance was normalized on a sapwood volume basis (Meinzer, 2003) confirming that variation in storage capacity can be quite extreme within a given environment (Holbrook et al. 2011). We know that structurally there is significant variation in the cellular arrangement of sapwood among coniferous, angiosperm ring porous and diffuse porous species, and that this structure changes over time from juvenile to mature wood (Holbrook et al. 2011). Because of this, looking at the density of these storage tissues may provide us with a more quantifiable framework for further understanding stored water release and embolism refilling amongst all woody species.

In response to the growing evidence emphasizing the tangled sequential and compensatory route of hydraulic failure in woody species, there has been a recent re-envisioning of the way we look at the plant hydraulics through the concept of the dynamic pipeline schematic (McCulloh et al. 2019; simplified version in Figure 1), with a new focus on keeping essential tissue hydrated before drought mortality occurs. As the field continues to expand upon its understanding of soil to leaf embolism resistance in plants, we are seeing an increase in evidence that supports the idea that the coordination of embolism refilling mechanisms routinely play a crucial role in maintaining low tissue water potential (Lachenbruch & McCulloh, 2014). This dynamic pipeline diagram (Fig. 1) is one of the first instances where attention to these tradeoffs is regarded as essential in the maintenance of hydraulic function at the cellular, tissue and whole plant scale. This pipeline schematic, proposed by McCulloh et al. (2019), highlights a wide variety of physiological, anatomical, and environmental factors at the leaf, stem, and root level that significantly influence hydraulic functioning. These properties are connected by either single-ended arrows, indicating causation, or double-ended arrows, indicating correlation, with associated plus and minus symbols representing positive or negative relationships (McCulloh et al. 2019). Many of the properties included in this diagram, such as stem hydraulic capacitance, woody habit, and hydraulic redistribution play an important role in influencing the parameters we use to measure hydraulic functioning (P50) but have not been addressed independently.

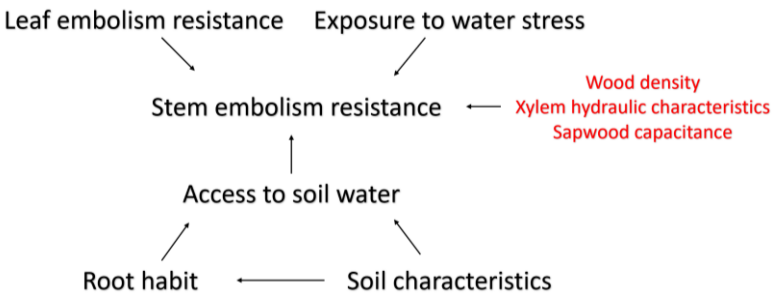

Figure 1. Simplified diagram of hydraulic pipeline paradigm (modified from McCulloh et. al 2019.) Arrows indicate direct causal relationships, and red text highlights the contribution and focus taken on in this study.

As a result of the McCulloh pipeline (2019), there have been recent calls to take a fresh look at whole-plant hydraulic function and include reliance on stored water as a crucial part of the puzzle (Körner 2019). The consequences of short-term water release from sapwood immediately affect the soil-plant-atmosphere continuum and ultimately determine when the water supply within the soil runs dry. Even as root hydraulic resistivity and osmotic potential decrease in an attempt to draw water into the root, at a certain point, the plant cannot access this diminishing amount of soil moisture (Larcher, 2003). As we continue to reassess whole plant hydraulic strategies more data is needed to better understand the stage in which a tree is fundamentally dependent on its own reserves of water following active soil dehydration. Inter-cellular rehydration from sapwood parenchyma can play a pivotal role in delaying this tissue dehydration until water deficit is relieved. Due to the significant contribution sapwood parenchyma makes in maintaining hydraulic flow (Körner 2019), I believe that sapwood capacitance could potentially provide a more detailed understanding as to when a tree will reach its point of critical tissue dehydration and resulting mortality.

An increased focus on sapwood capacitance and its relationship to wood density has led to research suggesting that they are causatively linked traits (Santiago et al. 2018, Gartner et al. 2005, Meinzer et al. 2008), especially when compared with additional xylem characteristics. The cost associated with producing xylem that is hydraulically efficient or embolism resistant is modified based on the needs of individuals to their given environment (Gleason et al. 2016), but the tradeoffs between structure and function are universally present across biome type (Lachenbruch & McCulloh, 2014). Xylem that is more resistant to embolism has greater conduit wall thickness and can withstand more negative water potentials, consequently decreasing the available space for sapwood parenchyma and other storage cell types (Hacke et al. 2001). This anatomical compromise in turn produces the relationship between wood density and sapwood capacitance (Santiago et al. 2018, Meinzer et al. 2010, Scholz et al. 2011). The purpose of this meta-analysis is to place sapwood capacitance and its relationship to wood density into the new hydraulic pipeline paradigm which describes the current framework used to organize the varying compensatory strategies plants use to maintain hydraulic efficiency. This robust and diverse (ecologically and functionally) data set will assist in evaluating the role that these tradeoffs play in the compensatory physiological reactions to water stress and allow for a more comprehensive understanding of all the hydraulic components related to drought survival.

Within this study I illuminate the functional importance of the relationship between sapwood density and sapwood capacitance. I look at this relationship on a

global scale and within individual biome types to understand variation in hydraulic relationships that is caused by differences in climate and use a structural equation model that builds on the hydraulic pipeline framework by adding sapwood density and capacitance (Figure 1). My goal is to demonstrate that considering compensatory mechanisms such as sapwood capacitance can improve predictions of plant drought responses that are based only on traditional methods. Based on the call to better recognize how sapwood pressure volume traits affect vulnerability to drought induced mortality (Santiago et al. 2018, Christoffersen et al. 2016), I explore sapwood trait values and relationships within and across biome types, growth forms, and phenology to ask: 1) How does density constrain or facilitate physiological function? 2) How do these constraints influence other trait properties that play a role in hydraulic efficiency? And 3) do morphological (phenology and growth form) or environmental aspects (mean annual temperature and precipitation) influence these properties? Answering these questions will provide insights into tradeoffs between safety and efficiency strategies, and provide a more detailed look at how sapwood capacitance and the use of stored water fit into both of these strategies.

Methods

I used pressure-volume curves to calculate sapwood capacitance and the five other hydraulic parameters (Table 3) we use to determine potential hydraulic strategy and functioning. Wood density was measured by using the water displacement method in order to identify the relationship and potential constraints that anatomy has on the observed hydraulic strategies and assemblages. Missing data for wood density was obtained from ICRAF's Tree Functional Attributes and Ecological Database (Harja et al. 2019). Data for P50 were not measured in this study but were collected and provided to us using the standard procedures (Sperry et al. 1988, Choat et al. 2010). For comparisons needed to understand whole plant strategy and the influence of environment, data for field sites was obtained from the WorldClim database.

Study Site and Species

I collected data from 7 sites (Table 1) for 34 species (Table 2). Fifteen species (Table 2) were collected during the rainy season of 2018 from the canopy crane located in an old-growth forest in the Parque Nacional San Lorenzo. This site is located on the Caribbean side of the Isthmus of Panama. The crane is equipped with a gondola suspended by cables from a rotating jib that allows access to about 0.8 ha of forest and is operated by the Smithsonian Tropical Research Institute in the Republic of Panama. An additional 19 species (Table 2) were collected from within the University of California Natural Reserve System. These reserves are natural ecosystems that are protected and

managed by the University of California for long term and undisturbed research. Site specific information can be found in Table 1.

Table 1. Site name, site code, latitude/longitude location, mean annual temperature (MAT), mean annual precipitation (MAP), elevation and soil type of field sites where branch collection occurred.

Site Name	Site Code	Lat/Long	MAT (°C)	MAP (cm)	Elevation (m)	Soil type
Angelo Coast Range Reserve	ACR	39.7, -123.7	11.5	203	140	Deep, well drained sandstone
Hastings Natural History Reserve	HNR	36.4, -121.6	17.0	53	142	Granite overlain by Miocene sedimentary section of syncline
McLaughlin Natural Reserve	MLR	38.9, -122.5	16.0	76	176	Scattered serpentine soils
Box Springs Reserve	BSR	33.9, -117.3	20.3	28	227	Biotite and granodiorite form a coarse-grained clay like soil
Santa Rosa Plateau Ecological Reserve	SRP	33.5, -117.2	15.0	78	443	Poorly drained basalt and limestone soil mixture
Scripps Coastal Reserve	SCR	32.8, -117.2	16.5	22	34	Shallow and dry serpentine soils
Stunt Ranch Reserve	STR	34.1, -118.6	20.1	610	125	Well drained clay loam soils
Parque National San Lorenzo, Panama	PAN	9.3, -79.9	26.0	1800	70	Dark brown alluvium underlain by a red sandstone subsoil

Table 2. Species, site code, mean (± 1 SD) π_o (MPa; sapwood osmotic potential at full turgor), ε (MPa; total sapwood bulk elastic modulus), θ_s ($m^3\ m^{-3}$; sapwood saturated water content), C_{ft} (kg m^3 $Mpa^{-1)}$; sapwood capacitance at full turgor), Ψ_{tlp} (MPa; sapwood water potential at turgor loss point), and RWC_{tlp} (total sapwood relative water content at turgor loss point), for 20 canopy trees and shrubs collected from the University of California Natural Reserve System and 15 canopy trees from Parque National San Lorenzo, Panama.

Species	Site	π_o	ε	θ_s	C_{ft}	Ψ_{tlp}	RWC_{tlp}
Ilex aquifolium	ACR	-1.76 ± 0.44	6.61 ± 1.99	0.63 ± 0.01	523.31 ± 189.17	-2.16 ± 0.42	77.18 ± 3.47
Notholithocarpus densiflorus	ACR	-1.15 ± 0.52	4.26 ± 1.04	0.51 ± 0.03	541.25 ± 65.49	-1.88 ± 0.67	67.55 ± 9.13
Picea abies	ACR	-1.15 ± 0.68	3.22 ± 1.60	0.78 ± 0.27	585.05 ± 58.53	-1.86 ± 0.69	61.56 ± 9.32
Quercus alba	ACR	-1.8 ± 0.18	4.67 ± 0.88	0.41 ± 0.06	470.25 ± 143.19	-2.37 ± 0.10	64.92 ± 2.31
Sequoia sempervirens	ACR	-0.51 ± 1.2	3.72 ± 0.87	0.61 ± 1.5	1180.79 ± 336.94	-2.13 ± 0.21	60.9 ± 8.43
Nicotiana glauca	ACR	-2.24 ± 0.77	3.68 ± 1.28	0.73 ± 0.25	545.34 ± 96.77	-2.66 ± 0.76	52.19 ± 8.01
Cupressus arizonica	HNR	-1.85 ± 0.14	6.83 ± 3.16	0.60 ± 0.05	254.17 ± 75.97	-2.50 ± 0.07	70.91 ± 10.44
Quercus chrysolepis	MLR	-0.56	0.86	0.60	360	-2.18	69.51
Encelia californica	SCR	-1.96 ± 0.02	7.47 ± 0.20	0.85 ± 0.01	49.79 ± 3.02	-3.05 ± 0.20	68.80 ± 5.82
Pittosporum tobira	MLR	-1.82 ± 0.46	3.75 ± 1.19	0.86 ± 0.06	384.78 ± 174.53	-2.39 ± 0.18	63.3 ± 2.74
Hedera algeriensis	STR	-0.93 ± 0.35	2.56 ± 0.08	1.00 ± 0.89	458.90 ± 248.04	-2.21 ± 0.02	37.68 ± 10.23
Cupressus Macrocarpa	MLR	-1.59 ± 0.58	9.38 ± 5.45	0.83 ± 0.27	571.32 ± 284.42	-2.50 ± 0.88	79.18 ± 13.14
Cassia grandis	SRP	-2.12 ± 0.09	8.07 ± 2.21	0.97 ± 0.03	58.65 ± 11.15	-2.99 ± 0.27	76.12 ± 6.69
Cotoneaster lacteus	STR	-2.33 ± 0.98	4.45 ± 1.84	0.71 ± 0.04	700.91 ± 167.43	-3.50 ± 1.04	62.46 ± 2.08
Rosa laevigata	HNR	-1.64 ± 0.07	3.44 ± 0.47	0.67 ± 0.02	55.67 ± 16.77	-2.38 ± 0.11	70.77 ± 3.85
Lantana trifolia	SRP	-1.15 ± 0.40	3.49 ± 0.98	1.11 ± 0.17	121.38 ± 50.80	-1.68 ± 0.58	76.58 ± 2.10
Schinus mole	BSR	-2.16 ± 0.28	4.28 ± 0.77	0.53 ± 0.14	114.85 ± 4.61	-2.63 ± 0.33	61.33 ± 3.61
Celtis occidentalis	BSR	-1.35 ± 0.14	5.01 ± 2.55	0.88 ± 0.09	754.68 ± 123.62	-2.27 ± 0.56	57.92 ± 2.54
Pittosporum tobira	SRP	-1.83 ± 0.46	3.75 ± 1.19	0.86 ± 0.06	384.78 ± 174.54	-2.39 ± 0.18	63.30 ± 2.74
Casspourea eliptIca	PAN	-1.89 ± 1.27	6.58 ± 23.93	0.58 ± 0.1	413.21 ± 61.65	-2.38 ± 1.01	48.15 ± 8.25
Ochroma pyramidale	PAN	-0.23	0.24	3.15	1118.00	-0.51	50.20
Poulsenia armata	PAN	-2.13 ± 0.40	4.34 ± 1.61	1.19 ± 0.26	488.33 ± 176.60	-2.69 ± 0.23	62.42 ± 2.12
Apeiba membranacea	PAN	-0.21	0.29	2.01	706	-0.65	47.10
Jacaranda copaia	PAN	-0.30 ± 0.06	0.49 ± 0.11	0.95 ± 0.35	473.1 ± 133.54	-0.95 ± 0.35	50.3 ± 4.75
Simarouba amara	PAN	-1.78 ± 0.28	3.14 ± 0.51	0.32 ± 0.01	399.76 ± 76.83	-2.08 ± 0.26	41.9 ± 0.07
Poruma bicolor	PAN	-0.60 ± 0.30	1.12 ± 0.61	1.28 ± 0.36	935.75 ± 313.34	-1.23 ± 0.53	45.87 ± 4.16
Trattinnickia aspera	PAN	-0.44	0.94	-	410	-0.63	74.1
Gustava superba	PAN	-1.45 ± 0.41	2.43 ± 0.69	3.59 ± 2.87	756.27 ± 11.73	-2.05 ± 0.28	40.18 ± 7.17
Calophyllum longifolium	PAN	-0.64 ± 0.28	4.10 ± 1.52	0.6 ± 0.01	476.53 ± 55.02	-1.25 ± 0.52	44.75 ± 1.34
Acalpha diversifolia	PAN	-1.75 ± 0.28	3.78 ± 1.65	0.62 ± 0.09	265.57 ± 39.65	-2.50 ± 0.37	45.5 ± 12.97
Palicourea guianensis	PAN	-2.79 ± 0.38	5.91 ± 1.03	0.66 ± 0.21	313.83 ± 10.57	-3.31 ± 0.25	40.3 ± 0.76
Virola elongata	PAN	-0.52	0.73	1.10	274	-1.5	49.40
Protium panamense	PAN	-1.42 ± 0.95	2.98 ± 1.21	0.60 ± 0.11	583.63 ± 61.39	-3.13 ± 0.70	48.78 ± 5.81
Nectandra purpurea	PAN	-1.30 ± 0.62	3.01 ± 0.11	0.60 ± 0.23	345.11 ± 85.90	-3.10 ± 0.19	60.91 ± 8.44

Xylem Capacitance & Sapwood Biophysical Properties

To determine hydraulic traits, a terminal branch from the canopy of each individual was collected between 0700 and 1000 hours for measurement of hydraulic parameters. Cut branches were sealed with parafilm and placed in black plastic bags containing saturated paper towels to prevent further transpiration from occurring. Samples were transported back to the laboratory facility within 3 hours. In the laboratory, 2 cm segments were cut from the branch and the bark and pith were removed, leaving behind a portion of fully hydrated xylem tissue for measurement of xylem water potential (Ψ). The initial mass of the tissue was taken on an analytical balance and placed inside a thermocouple psychrometer chamber (83 series; JRD Merrill Specialty Equipment, Logan, UT, USA) that was connected to a data logger (PSΨPRO; Wescor, Logan, UT, USA). The chambers were placed in a plastic bag and submerged in a water bath at 30°C for 3 hours to regulate air temperature in the chamber and achieve a stable reading. The dewpoint and microvolt output were measured, converted to MPa and recorded in 15-minute intervals. Samples were removed from the chambers every 3 hours, re-weighed, further dehydrated in a drying oven at 22°C for 5 minutes, and then resealed in the chambers for another 3 hours. This was repeated 5-7 times, until the samples reached a water potential of around -4.0 to -5.0 MPa. After the final Ψ was reached the xylem samples were then placed in a drying oven at 70°C for 36 hours to calculate final dry mass. Sapwood capacitance (kg m^{-3} Mpa^{-1}) was calculated as the slope

of the near linear portion in the initial part of the xylem water release curve (Meinzer et al. 2003).

Wood Density

For each stem that was used for hydraulic measurement, wood density was also measured. Samples were submerged in water for an hour to become saturated, and then were placed in a beaker of water on a scale. The mass of water displaced is equal to the volume of the sample. The sample was then dried in a drying oven at 70°C and after 48 hours the dry mass was measured. Wood density was calculated as the dry mass divided by the saturated weight volume (Chave, 2005).

Data Compilation

In addition to species (n=35) collected from our study sites (Table 1), we also assembled a dataset of water release curve parameters from the literature (n=228). The seven parameters (Table 3) were collected for woody species representing five biome types across continents with woody vegetation (Figure 1). All data available for desert biomes were collected on stem succulent species and could not be used. Values taken from the literature as well as raw data provided to us from collaborating researchers were included if the data collection was based on the same criteria and methods described previously in “Xylem Capacitance & Sapwood Biophysical Properties”. Species were used in the analysis if the study had measured change in mass and change in water potential of sapwood on a per volume basis. Climatic characteristics such as mean

annual temperature and mean annual precipitation were provided by the collaborators. Missing values were obtained from set of global climate layers (BioClim version 1.4, WorldClim).

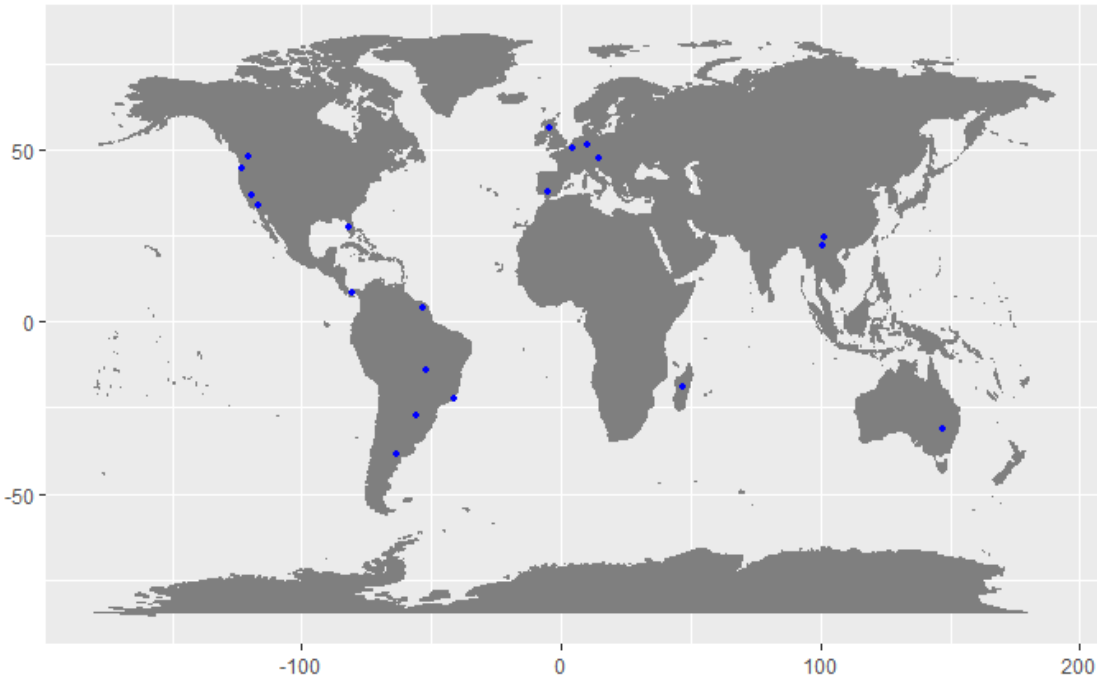

Figure 2. Map of locations where data was collected for the global analysis of hydraulic traits.

Statistical Analysis

Trait values were tested for normality and equal variance using a Shapiro-Wilk test in R, and all values met those assumptions. Additionally, bivariate trait relationships were analyzed with Pearson product–moment correlation using the Hmisc package in R. A quantile regression was used to quantify the upper limit of sapwood capacitance (C_{ft}) for a given wood density (ρ_w) using the quantreg package in R (Koenker, 2013).

From the pressure–volume curves, saturated water content (θs), osmotic potential at full turgor (π_o), water potential at turgor loss point (Ψ_{tlp}) and modulus of elasticity (ε) were calculated with the spreadsheet application by Sack and Pasquet-Kok (2011) according to methods described by Bartlett et al. (2012). Data points from three to four replicate curves per species were pooled. Species-specific values of sapwood capacitance (kg m^{-3} Mpa^{-1}) were taken as the slopes of linear regressions fitted to the initial phase of moisture release curves plotted as the cumulative mass of water released against sapwood water potential (Meinzer et al. 2003). Weight of water per unit tissue volume at saturation (kg m^{-3}) was calculated by multiplying the saturated/dry weight ratio of each tissue by tissue density (kg m^{-3}) and subtracting tissue density. The cumulative weight of water released per unit tissue volume was then calculated by multiplying the tissue relative water deficit at a given value of tissue water potential by the weight of water per unit tissue volume at saturation (Meinzer et al. 2008). Sapwood osmotic potential at zero turgor was estimated by plotting sapwood moisture release curves as pressure–volume curves then determining the transition points between the non-linear and linear portions of the curves (Meinzer et al. 2008).

Table 3. Symbols and descriptions of measured parameters.

Parameter	Description
θs	Saturated water content
π_o	Osmotic potential at full turgor
Ψ_{tlp}	Water potential at turgor loss point
ε	Bulk elastic modulus
RWC_{tlp}	Relative water content at turgor loss
C_{ft}	Sapwood capacitance
P50	50% loss of hydraulic conductivity
ρ_w	Sapwood Density

While I recognized that these methods were originally developed for use in leaves, recent use of this method to determine sapwood pressure volume traits has become more common, and all limitations and artifacts are considered and acknowledged accordingly (Meinzer et al. 2008, Sperry et al. 2008, Bucci et al. 2016). This technique only measured parenchymal capacitance and our samples were fully hydrated when measured, likely releasing water from the xylem and surrounding fibers, and steeply increasing the initial points of the pressure volume curve (Santiago et al. 2018). Additionally, traditional -1/Ψ method used to estimate leaf turgor loss point and bulk elastic modulus is not well established for xylem. This equation does not take into account an unknown but potentially significant amount of water draining from vessels (Tyree et al. 2003). Because of this, recent work from Brett Wolfe and Rick Meinzer has suggested that sapwood turgor loss be calculated from the “elbow of the cumulative water release curve (Meinzer et al. 2003, Pivovaroff personal communication). This “elbow” value was determined from instantaneous slopes of plots of cumulative water

released against sapwood water potential. These plots displayed a clear initial phase, in which cumulative water release decreased in logarithmic fashion as sapwood water potential declined up until a point (which we are further referring to as Ψ_{TLP}) where we saw a switch to a linear pattern of cumulative water release. In regards to the bulk elastic modulus of wood as inferred from stem shrinkage we must consider that the whole of the diameter of the xylem differentially contributed to elastic changes based on the specific tangential tensile or compressive stresses put on the cell wall of each individual tracheid or vessel (Irvine & Grace 1997). To account for these structural artifacts, recent approaches have elected to fit the data using an empirical fit with dehydration isotherms (Wolf & Kursar 2015, Tyree & Yang 1990). While we acknowledged these artifacts and potential limitations, the methods used to derive our parameters were chosen to be the best fit for the scope of this study.

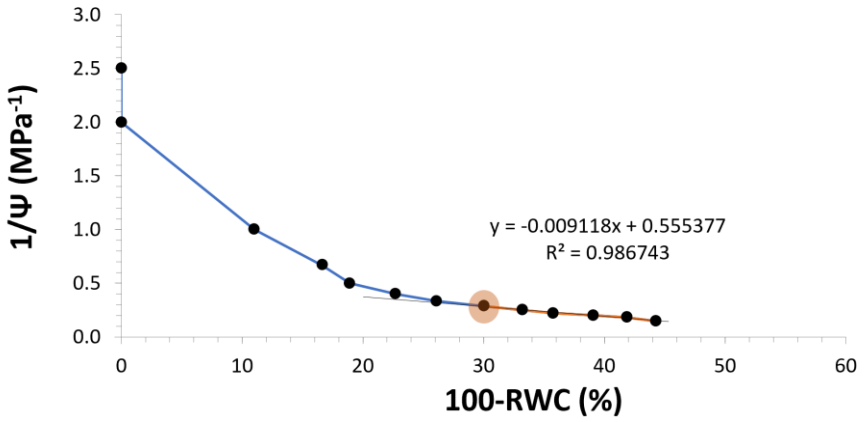

Figure 3. Sapwood pressure volume curve. The blue portion of the curve represents the initial logarithmic release of water, and the orange portion highlights the change to a linear dehydration phase. The orange circle highlights the F-elbow or turgor loss point, which we determine by choosing the best fitting slope and R^2 value of the regression run through the second phase of water release curve.

To determine if closely related species had similar trait values due to evolutionary history, I first built a pruned tree using TimeTree (Hedges et al. 2006). I then calculated Blomberg's K for each trait (Table 4). Blomberg's K is measure of phylogenetic signal that compares the observed signal in a trait to the signal under a Brownian motion model of trait evolution on a phylogeny (Blomberg et al. 2003). Values greater than one indicate a signal of phylogenetic conservatism (i.e., closely related species are more similar to each other than expected by random chance), while values closer to zero correspond to a pattern consistent with convergent evolution Revell, 2012, Diaz-Uriarte et al. 1996). The statistical significance of the phylogenetic signal is then evaluated using a null model of shuffling taxa labels across the tips of the phylogeny (Blomberg et al. 2003, Schreeg et al. 2010).

Table 4. Blomberg's K statistic from phylogenetic analysis of measured traits**.**

Parameter	K	p-value
θ_s	0.353	< 0.01
π_o	0.367	< 0.01
Ψ_{tlp}	0.351	< 0.01
ε	0.442	< 0.01
RWC_{tlp}	0.276	< 0.01
C_{ft}	0.554	< 0.01
P50	0.522	< 0.01
ρ_w	0.509	< 0.01

I used the lavaan package in R for the structural equation model analyses (Rosseel 2012) following guidelines outlined in (Petraitis et al. 1996, Grace et al. 2015). Our hypothesized models considered mean average temperature and mean average

precipitation the predictor variables that directly influenced $\rho_{w,}$ and their indirect relationship on ε, Ψ_{tlp}, and C_{ft} via their influence on ρ_w. While I recognize that soil physical characteristics can also play a significant role in influencing the measured traits in Table 4, these additional analyses were outside of the scope of the study. Multiple regressions were run to test the predictor variables for co-linearity, and there was significant covariation between mean annual precipitation and mean annual temperature with a value of 34.31 ($p < 0.001$). We found no collinearity in any other relationships between variables. Three potential models were created based on the logic of known general relationships between anatomy and physiology. These models were then tested against each other (Figure 7) until we found the best fitting relationship that satisfied all model fit indices. For each model, we removed variables to find the model with the lowest AIC, and then assessed model fit with a chi-square test, root mean square error of approximation (RMSEA) and goodness-of-fit index (GFI). Chi-square values with p-values < 0.05 and a RMSEA < 0.05 and GFI> 0.95 indicate a good model fit (Kline 2010, Grace et al. 2015). The path analysis was directed using the Lavaan package (Rosseel 2012), where the solid black arrows indicate significant direct relationships between predictor and outcome variables, and dotted arrows indicated negative significant relationships. We also acknowledge that while our data may fit well with our statistical model, that it only supports our interpretation of the process and does not imply true legitimacy of the process (McCune and Grace 2002).

Results

We found that there was a significant negative relationship between ρ_w and C_{ft} ($p < 0.001$) when looking across biomes for the globally pooled data. (Figure 4). The correlation matrix for that data (Table 5) showed that ρ_w, C_{ft} and ε were significantly correlated with all of the hydraulic parameters ($p < 0.001$). Additionally, almost all of the hydraulic variables were significantly correlated with one another, apart from P50, which was only correlated with ρ_w, ε, and Ψ_{tlp}. We further examined these relationships by also looking within biome (boreal, Mediterranean, savannah, temperate deciduous forest and tropical rainforest) (Figure 4). With density ellipses encompassing around 80% of the data points in each biome type, we saw distinct groupings of data points that suggest that environmental conditions could constrain these traits within a certain range (Figure 4). We then produced the same bi-variate regressions and correlation matrices within each of or five biomes (Table 6).

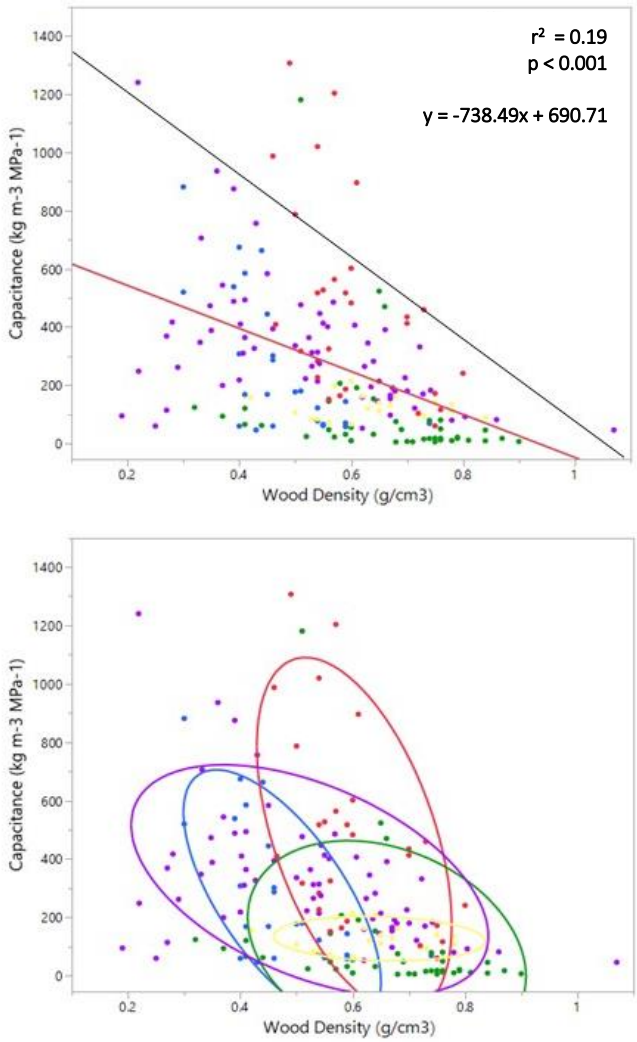

Figure 4. (Top) Relationship between wood density and sapwood capacitance across all biome types and (Bottom) Sapwood density and sapwood capacitance grouped by biome type with 0.8 density ellipses. Each point is the mean value of a species, r^2 values indicate coefficients of determination, the solid red line indicates the least squares regression, and the black line indicates the 0.95 quantile regression.

Table 5. Matrix of Pearson correlation coefficients for ρ_w (g/cm^3; sapwood density), P50 (MPa; water potential at fifty percent loss of conductivity), π_o (MPa; sapwood osmotic potential at full turgor), ε (MPa; total sapwood bulk elastic modulus), θ_s (m^3 m^{-3} ; sapwood saturated water content), C_{ft} (kg m^3 Mpa$^{-1)}$; sapwood capacitance at full turgor), Ψ_{tlp} (MPa; sapwood water potential at turgor loss point), and RWC_{tlp} (total sapwood relative water content at turgor loss point) for the global set of species (n=228).

	ρ_w	P50	π_o	ε	θ_s	C_{ft}	Ψ_{tlp}	RWC_{tlp}
ρ_w	1	-0.37*	-0.28*	0.24*	-0.40*	-0.42*	-0.33*	0.33*
P50		1	0.31	-0.54*	0.14	0.20	0.32*	-0.40*
π_o			1	-0.76*	0.21*	0.30*	0.83*	-0.44*
ε				1	-0.3*	-0.33*	-0.63*	0.50*
θ_s					1	0.27*	0.14	-0.43*
C_{ft}						1	0.29*	-0.34*
Ψ_{tlp}							1	-0.22*
RWC_{tlp}								1

The most significant and best fitting bivariate relationships for ρ_w and C_{ft} were found for the boreal, Mediterranean, and tropical rainforest biomes (Figure 5). Significant relationships within biome types also differed from the global average (Table 6) and varied in strength between biome types. Two traits of particular interest displayed inter-biome variation that led us to propose better sequential hypotheses when looking at our final structural equation models. Water potential at turgor loss point and ρ_w showed a tight correlation and high significance ($r^2 = 0.71$, $p < 0.01$) in the savannah biome, which had our highest average annual mean temperatures. Looking at this relationship in order of decreasing mean annual average temperature (savannah > tropical > temperate etc.) the direction and significance of this relationship decreased as the biome types became colder (Table 6). On the other hand, the relationship between C_{ft} and ε had a nonsignificant relationship across all biome types (Table 6).

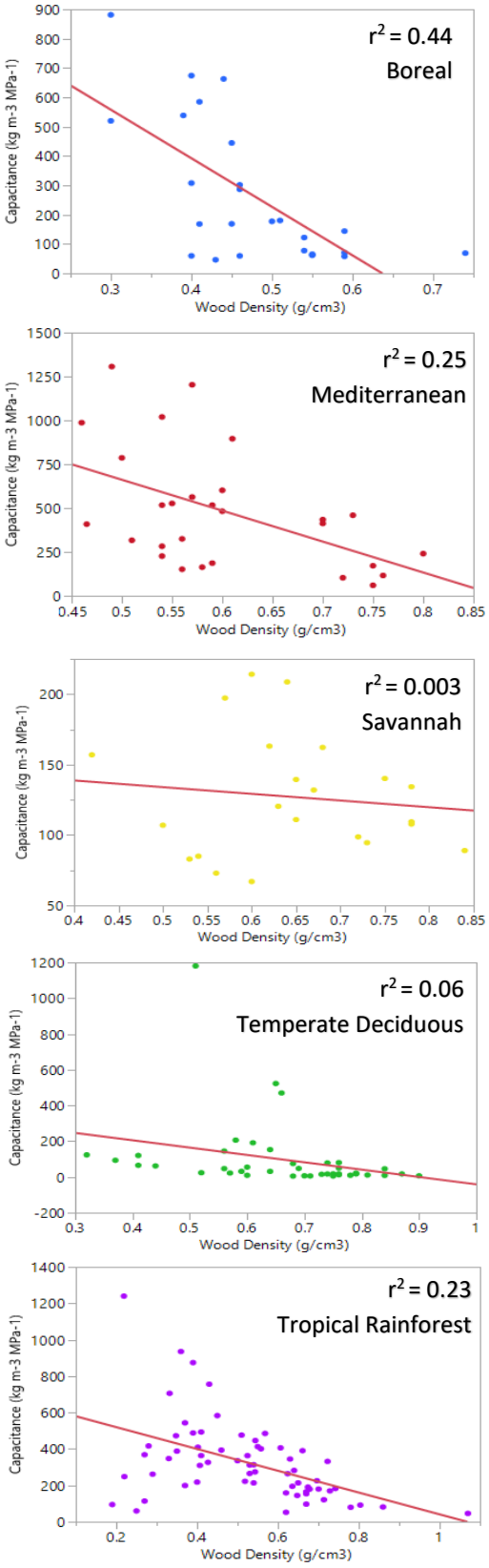

Figure 5. Bivariate relationship between wood density and sapwood capacitance subsetted by biome: Boreal, Mediterranean, Savannah, Temperate deciduous forest and Tropical rainforest.

Table 6. Matrix of Pearson correlation coefficents of relationships between ρ_w (g/cm^3; sapwood density), P50 (MPa; water potential at fifty percent loss of conductivity), π_o (MPa; sapwood osmotic potential at full turgor), ε (MPa; total sapwood bulk elastic modulus), θ_s (m^3 m^{-3} ; sapwood saturated water content), C_{ft} (kg m^3 Mpa$^{-1)}$; sapwood capacitance at full turgor), Ψ_{tlp} (MPa; sapwood water potential at turgor loss point), and RWC_{tlp} (total sapwood relative water content at turgor loss point) subsetted by biome: Mediterranean, savannah, temperate deciduous forest and tropical rainforest.

Mediterranean

	ρ_w	P50	π_o	ε	θ_s	C_{ft}	Ψ_{tlp}	RWC_{tlp}
ρ_w	1	-0.53	-0.06	0.30	-0.60*	-0.42*	-0.26	0.08
P50		1	0.64*	-0.84*	0.32	0.49	0.76	-0.14
π_o			1	-0.70*	0.65*	0.50*	0.76*	-0.49
ε				1	-0.23	-0.3	-0.69*	0.50*
θ_s					1	0.17	0.40	-0.03
C_{ft}						1	0.40*	-0.34*
Ψ_{tlp}							1	-0.23
RWC_{tlp}								1

Savannah

	ρ_w	P50	π_o	ε	θ_s	C_{ft}	Ψ_{tlp}	RWC_{tlp}
ρ_w	1	-	-0.70*	0.24	0.30	-0.06	0.71*	0.57
P50		1	-	-	-	-	-	-
π_o			1	0.54*	-0.36	0.26	0.97*	-0.50*
ε				1	-0.06	-0.21	-0.49*	0.12
θ_s					1	0.38	-0.41	0.25
C_{ft}						1	-0.26	0.18
Ψ_{tlp}							1	-0.43
RWC_{tlp}								1

Temperate Deciduous

	ρ_w	P50	π_o	ε	θ_s	C_{ft}	Ψ_{tlp}	RWC_{tlp}
ρ_w	1	-	-0.14	0.08	-0.05	-0.42*	-0.20	0.03
P50		1	-	-	-	-	-	-
π_o			1	-0.86	0.15	0.15	0.92*	0.50*
ε				1	-0.24	-0.15	-0.75*	0.60*
θ_s					1	-0.02	0.07	-0.24
C_{ft}						1	0.11	-0.18
Ψ_{tlp}							1	-.20

Tropical Rainforest

	ρ_w	P50	π_o	ε	θ_s	C_{ft}	Ψ_{tlp}	RWC_{tlp}
ρ_w	1	-0.33	0.02	0.06	-0.61*	-0.50*	0.01	0.27
p50		1	0.48	-0.61*	0.58	0.07	0.13	0.01
π_o			1	-0.70*	0.20	0.13	0.10	0.21
ε_x				1	-0.37*	-0.18	-0.48*	0.14
θ_s					1	0.55*	0.14	-0.46*
C_{ft}						1	0.40*	-0.48*
Ψ_{tlp}							1	0.19
RWC_{tlp}								1

I further examined potential causes of variation in the global distribution of both ρ_w and C_{ft} by comparing variation among biomes to variation in phenology (deciduous or evergreen) and growth form (liana, shrub or tree). The most significant differences in mean values of ρ_w and C_{ft} came from the differences in biome type, as compared to phenology and growth form (Figure 6). Phenology had no effect on these traits ($F = 1.29$; $p = 0.28$), and growth form only marginally affected wood density of shrubs, which had a higher average value than lianas and trees traits ($F = 8.38$; $p>0.05$). Similarly, I found that evolutionary history was not a key source of variation in the observed hydraulic variation. All K values were less than 0.37, but with p-values <0.001 (Table 4), reflecting that phylogenetic relationships have a weak but significant influence on the values of our measured traits.

The strong significant impact on ρ_w and C_{ft} associated with biome type led us to further explore the effect that environment (patterns of precipitation and temperature) had on these measured traits. We used three hypothesized models to determine if these variables were potentially driving underlying the variation among biomes. Our best fit model (Figure 7A) showed strong direct effects of precipitation and temperature on ρ_w, as well as significant indirect effects on ε. Additionally, ρ_w affected ε, ρ_w, and Ψ_{tlp}. Elasticity also very strongly influenced Ψ_{tlp} and had a negative relationship with ρ_w. This model had a Chi square value (x^2) of 5.58, a goodness of fit value of 0.988, and root square mean of error (RMSEA) of 0.05, indicating good model fit (Fan et al. 2007). We also note that while this model fits the data better than the other hypothesized

pathways, that it does not necessarily imply significance in causation, rather it logically suggests the directionality and sequence of relationships found in our data.

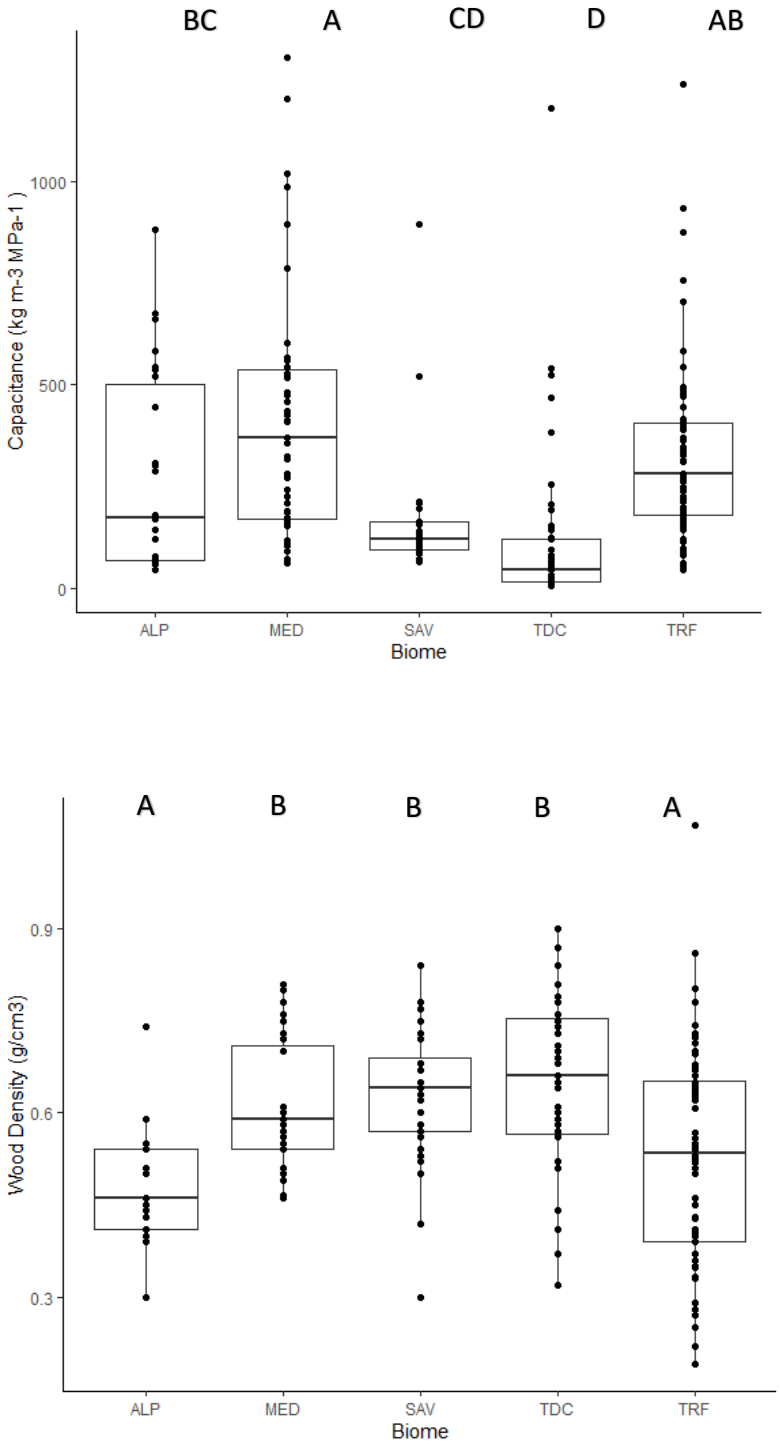

Figure 6. Box plots comparing global means (line inside box) and indicating the 25 and 75 percentiles (open bar) for sapwood capacitance (top) and sapwood density (bottom) between biome. Significant differences ($p < 0.05$) between means are indicated by different letters and were tested by running an ANOVA.

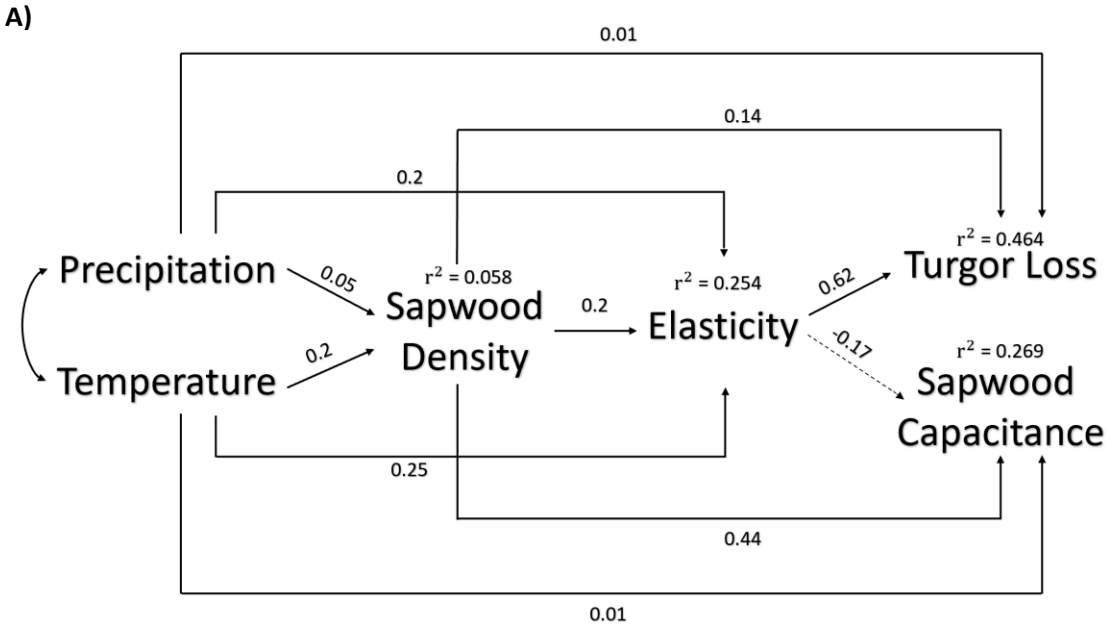

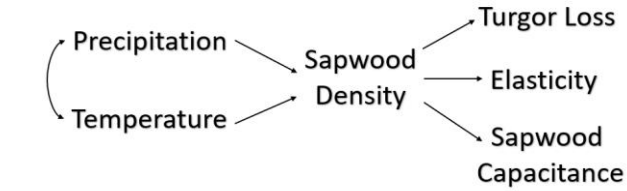

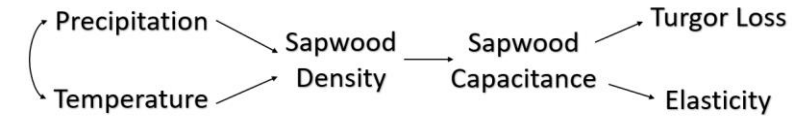

Figure 7. (A) Structural equation model demonstrating best fit causal relationships among mean annual precipitation and temperature, sapwood density, modulus of elasticity, water potential at turgor loss and sapwood capacitance. Values on lines represent the path coefficients of each relationship. (B) and (C) are alternative hypothesized models proposed and tested.

Table 7. Direct, indirect, and total (based on path analysis) of the predictor variables on sapwood capacitance (C_{ft}) and water potential at turgor loss (Ψ_{tlp}). Non-significant results are denoted with "ns".

Predictor	Pathway	Effect (pathway coefficient)	
		Ψ_{tlp}	C_{ft}
Precipitation	Direct	ns	ns
	Indirect through ρ_w	0.007	0.022
	Indirect through ε	0.124	-0.034
	Indirect through ρ_w and ε	0.062	-0.002
	Total	0.193	-0.014
Temperature	Direct	ns	ns
	Indirect through ρ_w	0.028	0.088
	Indirect through ε	0.155	-0.043
	Indirect through ρ_w and ε	0.025	-0.007
	Total	0.208	0.038
Wood Density	Direct	0.140	0.440
	Indirect through ε	0.124	-0.034
	Total	0.264	0.406

Discussion

My results for the global analysis showed that C_{ft}, as well as other water transport properties had an inverse relationship with ρ_w. Denser sapwood tended to result in lower π_o, θ_s, C_{ft}, Ψ_{tlp} and RWC_{tlp}. The relationship between ρ_w and C_{ft} had a significant negative linear relationship both at the global and individual biome scale (with the exception of the savannah biome). We think this could be potentially due to shrinking/swelling tendencies of woody species often observed in subtropical dry - season deciduous woody species (Avila-Lovera, 2018, Hinckley, 1975). The reoccurring support for the inverse relationship between C_{ft} and ρ_w we found within and between biome types suggests that ρ_w could be relied upon to better understand potential water storage capacity of an individual within any biome. My structural equation model also lends further support to the idea that this relationship, which many had previously claimed to be potentially just correlative, could be a result of direct anatomical and subsequently hydraulic tradeoffs. The statistical support for the inverse relationship between C_{ft} and ρ_w, coupled with additional support from our best fitting path analysis gives us increased confidence that we could use ρ_w as representative metric for inferring a variety of hydraulic and xylem characteristics within a species.

While many combinations of physiological and anatomical tradeoffs play a role in maintaining optimal sap flow (Enquist, 2002, Lachenbruch et al. 2018), the correlative trends I found in ε, Ψ_{tlp}, and C_{ft}, that were influenced by ρ_w supported two common functional strategies: safety vs. efficiency. This tradeoff is based on evidence that

indicates wider vessels will cavitate more frequently at less negative water potentials as compared to narrower vessels, and that maximum rate of water movement through vessels increases with their diameter (Martínez-Vilalta et al. 2002, Santiago et al. 2016). Species that have "efficient" xylem tend to have longer or wider xylem configurations, allowing for increased water transport capacity per cross-sectional stem area (Taneda & Sperry 2008). Efficient vessel configurations tend to result in lower wood densities (Taneda & Sperry 2008) and subsequently increased volume for water storage, which may compensate for their increased vulnerability to drought stress (Santiago et al. 2016). Many studies have demonstrated that woody species in tropical ecosystems tend to employ the "efficiency" strategy due to more frequent and stable periods of rainfall (Jansen et al. 2004). Additionally, we see that our subset of tropical data (Table 6) generally illustrates this strategy. With average values for ρ_w being much lower than species found in other biomes, the values for C_{ft} was much higher. Higher values of ε and its very significant relationship to low values of Ψ_{tlp} demonstrates that these species that move more water through their xylem, rely on their buffering capacity, as their Ψ_{tlp} is comparatively much higher than species found in drier ecosystem types (Borchert & Pockman 2005, Meinzer et al. 2008).

Species that employ the "safety" strategy constrain their vessel size in order to significantly decrease the value in which a certain water potential will cause cavitation (Tyree & Sperry, 1989, Mencuccini et al. 1997). Safety from this cavitation is dependent upon on the tightness of the capillary seal that averts air from leaking across pit

membranes and forming embolism (Lucas et al. 2013). And with support from the pit area hypothesis, we know that the as pit area increases, so does the probability that the pit seals will leak (Wheeler et al. 2005). This translates to “safer” species building narrower and smaller vessels, resulting in a generally denser sapwood structure. Denser sapwood decreases available space for stored water in surrounding parenchyma and fiber tissues, as well as reduces the elastic ability of that xylem. Denser sapwood, while also providing increased mechanical strength and higher resistance to xylem cavitation (Meinzer et al. 2003), is also strongly negatively correlated to Ψ_{tlp} and is a commonly found trait for species within drier ecosystems (Fu & Meinzer, 2019). We saw this pattern reflected in our data from both our savannah and Mediterranean type biomes (Table 6.). Overall, species from these drier sites saw much more negative water potentials before turgor loss occurred, alongside significant and tight correlations between cellular elasticity and turgor loss. Additionally, the RWC_{tlp} held a much more significant relationship with Ψ_{tlp} and ε.

So generally, species either have low ρ_w and high C_{ft} to buffer against daily or seasonal fluctuations in leaf and stem water status or they have a higher ρ_w, and rely on safer xylem configurations, resulting in a lower C_{ft} and a more negative Ψ_{tlp}. The architectural traits of the species are what determine the storage or safety strategy (Sperry et al. 2008, Poorter et al. 2010) and our SEM analysis alongside support from the literature (Lachenbruch et al. 2014, Meinzer et al. 2009, Hacke et al. 2001) suggests that the amalgamation of these traits is influenced by environmental variables

Diving father into these differences, we found the strength, significance and directionality of our hydraulic trait relationships observed on a global scale were not maintained in the individual biome analyses. In the temperate deciduous and savannah biomes, where average annual rainfall totals were more variable between sites, we saw non-significant relationships between ρ_w, $C_{ft,}$ and ε, but ρ_w was significantly related to Ψ_{tlp}. Conversely, in the three other biome types that experienced higher mean annual precipitation and more predictable seasonal precipitation and temperature fluctuations, Ψ_{tlp} had no significant relations with any sapwood variables but there were significant correlations between ρ_w, C_{ft} and ε. This further increases our belief that xylem structure and plant hydraulic strategy are ultimately influencing Ψ_{tlp}, which remains a key trait in the sequence of plant drought responses (Bartlett et al. 2016). Mean C_{ft} values were also significantly different from each other between biome type (Table 6) but average sapwood density was only significant between the two biome types with the largest mean annual temperature differences. These results suggested that environmental variability may consequently constrain the arrangement and the sequential importance of these traits.

In addition to evaluating the environmental influence on our hydraulic traits, we also tested the phylogenetic signal between species to account for any evolutionary history that may cause related species to resemble each other. Our use of Blomberg's K allows us to compare species average trait values across different trees to potentially uncover similarities in traits due to evolutionary patterns (Blomberg et al. 2003). Our

results from this analysis (Table 4) indicate a twofold conclusion that all our traits showed low phylogenetic signal, and that this low signal is significant under multiple randomization tests (Blomberg et al. 2003). The K values for all of our traits fall closer to zero, suggesting that relatives resemble each other less than what is expected under Brownian motion evolution (Adams, 2014). This leads us to believe that the mean values of these species' hydraulic traits are not determined by some other adaptive evolution that is related to the phylogeny (Ackerley, 2009). The low p-values associated with the K statistics additionally supports our use of randomization tests to test whether our K parameter is statistically different from zero (Blomberg et al. 2003, Garland personal communication).

Having explored variation in strategies between biome type, across taxa, and within distinct environmental groupings, our data suggest that the environment possibly will play a significant role in determining hydraulic performance. Because of this, in our final model (Figure 7A) we hypothesized that climatic variables had significant direct effects on ρ_w, which would ultimately determine the strategy of the individual and its capability to utilize stored water. We proposed in this final model that the two exogenous variables (mean annual precipitation and mean annual temperature) and the subsequent predicted trait values were determined by these two forcing variables and the hypothesized cause–effect linkages between them (Vile et al. 2006). Climate directly affected ρ_w, but indirectly affected ε, again reiterating this reoccurring tradeoff we see between strength and storage. Our strongest predictor in the model is ρ_w (Table 7.) the

initial measured trait in the sequence that then directly influenced ε, C_{ft}, and Ψ_{tlp}. Additionally, ε played a direct role in influencing both turgor loss point and sapwood capacitance. Our model provides the best hypothesis to address the role of environment in influencing trait values, while simultaneously recognizing that anatomy (ρ_w) also impacts those values. While this schematic seems biologically and physiologically logical, path analysis is crucial in defining and providing statistical support for direct and indirect relationships and identifying the sequence of these relationships. This model does not include all of the collected and measured variables within our database but allows us to place our focus on C_{ft} and ρ_w within the larger context of climate and environment.

Conclusion

In this study we show that ρ_w is related to C_{ft} and the amount of stored water potentially available for preventing embolism. At the physiological level, these two traits, and the relationship between them also influence and constrain other hydraulic trait properties that play a role in maintaining hydraulic efficiency. At the phylogenetic scale we found that closely related species did not necessarily have similar trait values due to Brownian evolutionary expectations. At the biome level our path analysis shows that environment, as dictated by mean annual precipitation and temperature, plays a significant role in influencing the sequence and overall hydraulic strategy used by an individual within its habitat. Having a framework that provides a structured understanding of these tradeoffs and relationships at the global and ecosystem level, in addition to analyses of hydraulic relationships at the cellular level provides us with increased understating of how trait combinations fit into the safety vs. efficiency tradeoff.

As we continue to refine our understanding of drought induced tree mortality, and the role that maintaining hydraulic efficiency plays in this phenomenon, having access to a robust and diverse database for these types of analyses becomes increasingly important. Explicit understanding of the mechanistic basis of these processes will eventually allow us to quantify and understand vulnerability to drought mortality from the cellular scale, up to the ecosystem level. Our results, along with an increase in the collection of this type of sapwood data, will facilitate the use of

potentially more accurate metrics to be used in management and conservation of at-risk ecosystems. Our study provides increased evidence that previously used predictor variables (such as P50) may not represent species risk as accurately as C_{ft}. Continued support for the negative linear relationship between sapwood capacitance and sapwood density, continues the conversation for using ρ_w as a reliable morphometric trait to estimate the buffering capacity and potential stress resistance of a species within a given environment.

The novelty of this study stems from the number and variety of different species for which sapwood traits and relationships were analyzed. While there is widespread open access to robust databases of leaf pressure volume traits, we are now seeing an increased importance in collecting these pressure volume traits for sapwood. Future efforts in continuing the pursuit of these goals should also focus on collecting sapwood hydraulic data for woody species in increasingly more specific biome types (tropical could be split into tropical rainforest vs. tropical seasonal forest). As species ranges shift over time, there is increased opportunity for furthering our understanding of these relationships by including other variables such as elevation and soil type to this analysis. Additionally, as we continue to measure these parameters for sapwood, the methods and equations used for calculating the trait values will become honed and may find increased methodological support.

Our results found at all functional levels (cellular, vascular, and ecosystem) place hydraulic maintenance in more well-defined position in the context climate change. On

a general level we define how environment affects sapwood anatomy, and how subsequently sapwood anatomy influences hydraulic function. The patterns we found in hydraulic function continue to support the safety vs. efficiency tradeoff and indicate that phylogeny, growth form, and leaf habit do not play a strong role in influencing any of these properties. As the climate continues to change globally and locally, our perspectives from this study, alongside our structural equation model may provide a more accurate and easier procedure to look at species vulnerability to drought mortality.

Literature Cited

Ackerly, D. (2009). Conservatism and diversification of plant functional traits: evolutionary rates versus phylogenetic signal. *Proceedings of the National Academy of Sciences*, *106*(Supplement 2), 19699-19706.

Adams, D. C. (2014). A generalized K statistic for estimating phylogenetic signal from shape and other high-dimensional multivariate data. *Systematic Biology*, *63*(5), 685-697.

Allen, C. D., Macalady, A. K., Chenchouni, H., Bachelet, D., McDowell, N., Vennetier, M., ... & Gonzalez, P. (2010). A global overview of drought and heat-induced tree mortality reveals emerging climate change risks for forests. *Forest Ecology and Management*, *259*(4), 660-684.

Anderegg, W. R., Klein, T., Bartlett, M., Sack, L., Pellegrini, A. F., Choat, B., & Jansen, S. (2016). Meta-analysis reveals that hydraulic traits explain cross-species patterns of drought-induced tree mortality across the globe. *Proceedings of the National Academy of Sciences*, *113*(18), 5024-5029.

Avila Lovera, E. (2018). *Do Plants With Photosynthetic Stems Respond Differently to Drought? An Ecophysiological Evaluation of Desert Communities* (Doctoral dissertation, UC Riverside).

Barnard, D. M., Meinzer, F. C., Lachenbruch, B., McCulloh, K. A., Johnson, D. M., & Woodruff, D. R. (2011). Climate-related trends in sapwood biophysical properties in two conifers: avoidance of hydraulic dysfunction through coordinated adjustments in xylem efficiency, safety and capacitance. *Plant, Cell & Environment*, *34*(4), 643-654.

Bartlett, M. K., Klein, T., Jansen, S., Choat, B., & Sack, L. (2016). The correlations and sequence of plant stomatal, hydraulic, and wilting responses to drought. *Proceedings of the National Academy of Sciences*, *113*(46), 13098-13103.

Bartlett, M. K., Scoffoni, C., & Sack, L. (2012). The determinants of leaf turgor loss point and prediction of drought tolerance of species and biomes: a global meta-analysis. *Ecology Letters*, *15*(5), 393-405.

Benjamini, Y., & Hochberg, Y. (2000). On the adaptive control of the false discovery rate in multiple testing with independent statistics. *Journal of educational and Behavioral Statistics*, *25*(1), 60-83.

Blomberg, S. P., Garland Jr, T., & Ives, A. R. (2003). Testing for phylogenetic signal in comparative data: behavioral traits are more labile. *Evolution*, *57*(4), 717-745.

Borchert, R., & Pockman, W. T. (2005). Water storage capacitance and xylem tension in isolated branches of temperate and tropical trees. *Tree Physiology*, *25*(4), 457-466.

Bucci, S. J., Scholz, F. G., Campanello, P. I., Montti, L., Jimenez-Castillo, M., Rockwell, F. A., ... & Enricci, J. (2012). Hydraulic differences along the water transport system of South American Nothofagus species: do leaves protect the stem functionality?. *Tree Physiology*, *32*(7), 880-893.

Bucci, S. J., Goldstein, G., Scholz, F. G., & Meinzer, F. C. (2016). Physiological significance of hydraulic segmentation, nocturnal transpiration and capacitance in tropical trees: Paradigms revisited. In *Tropical Tree Physiology* (pp. 205-225). Springer, Cham.

Chave, J. (2005). Measuring wood density for tropical forest trees. *A field manual for the CTFS sites*, 1-7.

Chiang, J. M., Spasojevic, M. J., Muller-Landau, H. C., Sun, I. F., Lin, Y., Su, S. H., ... & McEwan, R. W. (2016). Functional composition drives ecosystem function through multiple mechanisms in a broadleaved subtropical forest. *Oecologia*, *182*(3), 829-840.

Choat, B., Drayton, W. M., Brodersen, C., Matthews, M. A., Shackel, K. A., Wada, H., & McElrone, A. J. (2010). Measurement of vulnerability to water stress-induced cavitation in grapevine: a comparison of four techniques applied to a long-vesseled species. *Plant, Cell & Environment*, *33*(9), 1502-1512.

Choat, B., Brodribb, T. J., Brodersen, C. R., Duursma, R. A., López, R., & Medlyn, B. E. (2018). Triggers of tree mortality under drought. *Nature*, *558*(7711), 531-539.

Christoffersen, B. O., Gloor, M., Fauset, S., Fyllas, N. M., Galbraith, D. R., Baker, T. R., ... & Sevanto, S. (2016). Linking hydraulic traits to tropical forest function in a size-structured and trait-driven model (TFS v. 1-Hydro). Geoscientific Model Development.

De Guzman M.E., Acosta-Rangel, A., Winter, K., Meinzer, F. C., Damien Bonal, D., Santiago, L. S. (submitted) Hydraulic traits of Neotropical canopy liana and tree species across a broad range of wood density: implications for drought mortality models. *Tree Physiology*.

De Guzman, M. E., Santiago, L. S., Schnitzer, S. A., & Álvarez-Cansino, L. (2017). Trade-offs between water transport capacity and drought resistance in neotropical canopy liana and tree species. *Tree Physiology*, *37*(10), 1404-1414.

Diaz-Uriarte, R., & Garland Jr, T. (1996). Testing hypotheses of correlated evolution using phylogenetically independent contrasts: sensitivity to deviations from Brownian motion. *Systematic Biology*, *45*(1), 27-47.

Enquist, B. J. (2002). Universal scaling in tree and vascular plant allometry: toward a general quantitative theory linking plant form and function from cells to ecosystems. *Tree Physiology*, *22*(15-16), 1045-1064.

Fan, X., & Sivo, S. A. (2007). Sensitivity of fit indices to model misspecification and model types. *Multivariate Behavioral Research*, *42*(3), 509-529.

Feild, T. S., & Brodribb, T. J. (2013). Hydraulic tuning of vein cell microstructure in the evolution of angiosperm venation networks. *New Phytologist*, *199*(3), 720-726.

Fu, X., & Meinzer, F. C. (2019). Metrics and proxies for stringency of regulation of plant water status (iso/anisohydry): a global data set reveals coordination and trade-offs among water transport traits. *Tree Physiology*, *39*(1), 122-134.

Fu, X., Meinzer, F. C., Woodruff, D. R., Liu, Y. Y., Smith, D. D., McCulloh, K. A., & Howard, A. R. (2019). Coordination and trade-offs between leaf and stem hydraulic traits and stomatal regulation along a spectrum of isohydry to anisohydry. *Plant, Cell & Environment*, *42*(7), 2245-2258.

Gartner, B. L., & Meinzer, F. C. (2005). Structure-function relationships in sapwood water transport and storage. In *Vascular transport in plants* (pp. 307-331). Academic Press.

Gleason, S. M., Westoby, M., Jansen, S., Choat, B., Hacke, U. G., Pratt, R. B., ... & Cochard, H. (2016). Weak tradeoff between xylem safety and xylem-specific hydraulic efficiency across the world's woody plant species. *New Phytologist*, *209*(1), 123-136.

Grace, J. B., Scheiner, S. M., & Schoolmaster Jr, D. R. (2015). Structural equation modeling: building and evaluating causal models: Chapter 8.

Hacke, U. G., Sperry, J. S., Pockman, W. T., Davis, S. D., & McCulloh, K. A. (2001). Trends in wood density and structure are linked to prevention of xylem implosion by negative pressure. *Oecologia*, *126*(4), 457-461.

Hammond, W. M., Yu, K., Wilson, L. A., Will, R. E., Anderegg, W. R., & Adams, H. D. (2019). Dead or dying? Quantifying the point of no return from hydraulic failure in drought-induced tree mortality. *New Phytologist*, *223*(4), 1834-1843.

Harja, D., Rahayu, S., & Pambudi, S. (2019). Tree functional attributes and ecological database. http://db.worldagroforestry.org/.

Hedges, S. B., Dudley, J., & Kumar, S. (2006). TimeTree: a public knowledge-base of divergence times among organisms. *Bioinformatics*, *22*(23), 2971-2972.

Hinckley, T. M., & Bruckerhoff, D. N. (1975). The effects of drought on water relations and stem shrinkage of Quercus alba. *Canadian Journal of Botany*, *53*(1), 62-72.

Holbrook, N. M. (1995). Stem Water Storage. In *Plant Stems Physiology and Functional Morphology* (pp. 151-174). Academic Press; San Diego, CA.

Holbrook, N. M., & Zwieniecki, M. A. (Eds.). (2011). *Vascular transport in plants*. Elsevier; Burlington, MA.

Holbrook, N. M., & Sinclair, T. R. (1992). Water balance in the arborescent palm, Sabal palmetto. I. Stem structure, tissue water release properties and leaf epidermal conductance. *Plant, Cell & Environment*, *15*(4), 393-399.

Hölttä, T., Cochard, H., Nikinmaa, E., & Mencuccini, M. (2009). Capacitive effect of cavitation in xylem conduits: results from a dynamic model. *Plant, Cell & Environment*, *32*(1), 10-21.

Irvine, J., & Grace, J. (1997). Continuous measurements of water tensions in the xylem of trees based on the elastic properties of wood. *Planta*, *202*(4), 455-461.

Jansen, S., Baas, P., Gasson, P., Lens, F., & Smets, E. (2004). Variation in xylem structure from tropics to tundra: evidence from vestured pits. *Proceedings of the National Academy of Sciences*, *101*(23), 8833-8837.

Jupa, R., Plavcová, L., Gloser, V., & Jansen, S. (2016). Linking xylem water storage with anatomical parameters in five temperate tree species. *Tree Physiology*, *36*(6), 756-769.

Kembel, S. W., Cowan, P. D., Helmus, M. R., Cornwell, W. K., Morlon, H., Ackerly, D. D., ... & Webb, C. O. (2010). Picante: R tools for integrating phylogenies and ecology. *Bioinformatics*, *26*(11), 1463-1464.

Kline, R. B. (2015). *Principles and practice of structural equation modeling*. Guilford publications.

Koenker, R. (2013). quantreg: Quantile Regression. R package version 5.05. *R Foundation for Statistical Computing: Vienna) Available at: http://CRAN. R-project. org/package= quantreg*.

Körner, C. (2019). No need for pipes when the well is dry—a comment on hydraulic failure in trees. *Tree Physiology*, *39*(5), 695-700.

Lachenbruch, B., & McCulloh, K. A. (2014). Traits, properties, and performance: how woody plants combine hydraulic and mechanical functions in a cell, tissue, or whole plant. *New Phytologist*, *204*(4), 747-764.

Larcher, W. (2003). *Physiological plant ecology: ecophysiology and stress physiology of functional groups*. Springer Science & Business Media.

López-Bernal, Á., Alcántara, E., & Villalobos, F. J. (2014). Thermal properties of sapwood of fruit trees as affected by anatomy and water potential: errors in sap flux density measurements based on heat pulse methods. *Trees*, *28*(6), 1623-1634.

Lucas, W. J., Groover, A., Lichtenberger, R., Furuta, K., Yadav, S. R., Helariutta, Y., ... & Patrick, J. W. (2013). The plant vascular system: evolution, development and functions f. *Journal of Integrative Plant Biology*, *55*(4), 294-388.

Machado, J. L., & Tyree, M. T. (1994). Patterns of hydraulic architecture and water relations of two tropical canopy trees with contrasting leaf phenologies: Ochroma pyramidale and Pseudobombax septenatum. *Tree Physiology*, *14*(3), 219-240.

Manzoni, S., Katul, G., & Porporato, A. (2014). A dynamical system perspective on plant hydraulic failure. *Water Resources Research*, *50*(6), 5170-5183.

Martínez-Vilalta, J., Prat, E., Oliveras, I., & Piñol, J. (2002). Xylem hydraulic properties of roots and stems of nine Mediterranean woody species. *Oecologia*, *133*(1), 19-29.

McCulloh, K. A., Domec, J. C., Johnson, D. M., Smith, D. D., & Meinzer, F. C. (2019). A dynamic yet vulnerable pipeline: Integration and coordination of hydraulic traits across whole plants. *Plant, Cell & Environment*, *42*(10), 2789-2807.

McCulloh, K. A., Johnson, D. M., Meinzer, F. C., & Woodruff, D. R. (2014). The dynamic pipeline: hydraulic capacitance and xylem hydraulic safety in four tall conifer species. *Plant, Cell & Environment*, *37*(5), 1171-1183.

McCune, B., Grace, J. B., & Urban, D. L. (2002). *Analysis of ecological communities* (Vol. 28). Gleneden Beach, OR: MjM software design.

Meinzer, F. C., & McCulloh, K. A. (2013). Xylem recovery from drought-induced embolism: where is the hydraulic point of no return? *Tree Physiology*, *33*(4), 331-334.

Meinzer, F. C., McCulloh, K. A., Lachenbruch, B., Woodruff, D. R., & Johnson, D. M. (2010). The blind men and the elephant: the impact of context and scale in evaluating conflicts between plant hydraulic safety and efficiency. *Oecologia*, *164*(2), 287-296.

Meinzer, F. C. (2003). Functional convergence in plant responses to the environment. *Oecologia*, *134*(1), 1-11.

Meinzer, F. C., Woodruff, D. R., Domec, J. C., Goldstein, G., Campanello, P. I., Gatti, M. G., & Villalobos-Vega, R. (2008). Coordination of leaf and stem water transport properties in tropical forest trees. *Oecologia*, *156*(1), 31-41.

Meinzer, F. C., James, S. A., Goldstein, G., & Woodruff, D. (2003). Whole-tree water transport scales with sapwood capacitance in tropical forest canopy trees. *Plant, Cell & Environment*, *26*(7), 1147-1155.

Meinzer, F. C., Johnson, D. M., Lachenbruch, B., McCulloh, K. A., & Woodruff, D. R. (2009). Xylem hydraulic safety margins in woody plants: coordination of stomatal control of xylem tension with hydraulic capacitance. *Functional Ecology*, *23*(5), 922-930.

Mencuccini, M., and J. Comstock. "Vulnerability to cavitation in populations of two desert species, Hymenoclea salsola and Ambrosia dumosa, from different climatic regions." *Journal of Experimental Botany* 48.6 (1997): 1323-1334.

Mencuccini, M., Manzoni, S., & Christoffersen, B. (2019). Modelling water fluxes in plants: from tissues to biosphere. *New Phytologist*, *222*(3), 1207-1222.

Mencuccini, M., Minunno, F., Salmon, Y., Martínez-Vilalta, J., & Hölttä, T. (2015). Coordination of physiological traits involved in drought-induced mortality of woody plants. *New Phytologist*, *208*(2), 396-409.

Oliva Carrasco, L., Bucci, S. J., Di Francescantonio, D., Lezcano, O. A., Campanello, P. I., Scholz, F. G., ... & Holbrook, N. M. (2015). Water storage dynamics in the main stem of subtropical tree species differing in wood density, growth rate and life history traits. *Tree Physiology*, *35*(4), 354-365.

Passioura, J. B. (1982). Water in the soil-plant-atmosphere continuum. In *Physiological Plant Ecology II* (pp. 5-33). Springer, Berlin, Heidelberg.

Perämäki, M., Nikinmaa, E., Sevanto, S., Ilvesniemi, H., Siivola, E., Hari, P., & Vesala, T. (2001). Tree stem diameter variations and transpiration in Scots pine: an analysis using a dynamic sap flow model. *Tree Physiology*, *21*(12-13), 889-897.

Petraitis, P. S., Dunham, A. E., & Niewiarowski, P. H. (1996). Inferring multiple causality: the limitations of path analysis. *Functional ecology*, 421-431.

Pivovaroff, A. L., Pasquini, S. C., De Guzman, M. E., Alstad, K. P., Stemke, J. S., & Santiago, L. S. (2016). Multiple strategies for drought survival among woody plant species. *Functional Ecology*, *30*(4), 517-526.

Poorter, L., McDonald, I., Alarcón, A., Fichtler, E., Licona, J. C., Peña-Claros, M., ... & Sass-Klaassen, U. (2010). The importance of wood traits and hydraulic conductance for the performance and life history strategies of 42 rainforest tree species. *New Phytologist*, *185*(2), 481-492.

Pratt, R. B., Jacobsen, A. L., Ewers, F. W., & Davis, S. D. (2007). Relationships among xylem transport, biomechanics and storage in stems and roots of nine Rhamnaceae species of the California chaparral. *New Phytologist*, *174*(4), 787-798.

Revell, I. (2012). Phylogenetic signal with *K* and λ. *Phylogenitic Tools for Comparative Biology*. http://blog.phytools.org/

Richards, A. E., Wright, I. J., Lenz, T. I., & Zanne, A. E. (2014). Sapwood capacitance is greater in evergreen sclerophyll species growing in high compared to low-rainfall environments. *Functional Ecology*, *28*(3), 734-744.

Rosado, B. H. P., & De Mattos, E. A. (2010). Interspecific variation of functional traits in a CAM-tree dominated sandy coastal plain. *Journal of Vegetation Science*, *21*(1), 43-54.

Rosner, S., Heinze, B., Savi, T., & Dalla-Salda, G. (2019). Prediction of hydraulic conductivity loss from relative water loss: new insights into water storage of tree stems and branches. *Physiologia Plantarum*, *165*(4), 843-854.

Rosseel, Y. (2012). Lavaan: An R package for structural equation modeling and more. Version 0.5–12 (BETA). *Journal of Statistical Software*, *48*(2), 1-36.

Sack, L., Pasquet-Kok, J., & PrometheusWiki Contributors. (2011). Leaf pressure-volume curve parameters. *PrometheusWiki website: http://prometheuswiki. publish. csiro. au/tikiindex. php*.

Santiago, L. S., De Guzman, M. E., Baraloto, C., Vogenberg, J. E., Brodie, M., Hérault, B., ... & Bonal, D. (2018). Coordination and trade-offs among hydraulic safety, efficiency and drought avoidance traits in Amazonian rainforest canopy tree species. *New Phytologist*, *218*(3), 1015-1024.

Santiago, L. S., Bonal, D., De Guzman, M. E., & Ávila-Lovera, E. (2016). Drought survival strategies of tropical trees. In *Tropical Tree Physiology* (pp. 243-258). Springer, Cham.

Santiago, L. S., Acosta-Rangel, A., Avila-Lovera, E., Bucior, E., de Guzman, M. E., Meinzer, F. C., ... & Winter, K. (2019, December). Predicting drought responses of tropical woody plants through coordination among drought survival traits. In *AGU Fall Meeting 2019*. AGU.

Scholz, F. G., Bucci, S. J., Goldstein, G., Meinzer, F. C., Franco, A. C., & Miralles-Wilhelm, Fernando (2007). Biophysical properties and functional significance of stem water storage tissues in Neotropical savanna trees. *Plant, Cell & Environment*, *30*(2), 236-248.

Scholz, F. G., Phillips, N. G., Bucci, S. J., Meinzer, F. C., & Goldstein, G. (2011). Hydraulic capacitance: biophysics and functional significance of internal water sources in relation to tree size. In *Size-and age-related changes in tree structure and function* (pp. 341-361). Springer, Dordrecht.

Schreeg, L. A., Kress, W. J., Erickson, D. L., & Swenson, N. G. (2010). Phylogenetic analysis of local-scale tree soil associations in a lowland moist tropical forest. *PLoS One*, *5*(10).

Schweingruber, F. H., Börner, A., & Schulze, E. D. (2007). *Atlas of woody plant stems: evolution, structure, and environmental modifications*. Springer Science & Business Media.

Siddiq, Z., Zhang, Y. J., Zhu, S. D., & Cao, K. F. (2019). Canopy water status and photosynthesis of tropical trees are associated with trunk sapwood hydraulic properties. *Plant Physiology and Biochemistry*, *139*, 724-730.

Spasojevic, M. J., Grace, J. B., Harrison, S., & Damschen, E. I. (2014). Functional diversity supports the physiological tolerance hypothesis for plant species richness along climatic gradients. *Journal of Ecology*, *102*(2), 447-455.

Sperry, J. S., Donnelly, J. R., & Tyree, M. T. (1988). A method for measuring hydraulic conductivity and embolism in xylem. *Plant, Cell & Environment*, *11*(1), 35-40.

Sperry, J. S. (2003). Evolution of water transport and xylem structure. *International Journal of Plant Sciences*, *164*(S3), S115-S127.

Sperry, John S., Frede Sperry, J. S., Meinzer, F. C., & McCulloh, K. A. (2008). Safety and efficiency conflicts in hydraulic architecture: scaling from tissues to trees. *Plant, Cell & Environment*, *31*(5), 632-645.

Taneda, H., & Sperry, J. S. (2008). A case-study of water transport in co-occurring ring-versus diffuse-porous trees: contrasts in water-status, conducting capacity, cavitation and vessel refilling. *Tree Physiology*, *28*(11), 1641-1651.

Tyree, M. T., & Sperry, J. S. (1989). Vulnerability of xylem to cavitation and embolism. *Annual Review of Plant Biology*, *40*(1), 19-36.

Tyree, M. T., & Zimmermann, M. H. (2002). Hydraulic architecture of whole plants and plant performance. In *Xylem Structure and the Ascent of Sap* (pp. 175-214). Springer, Berlin, Heidelberg.

Tyree, M. T., Cochard, H., & Cruiziat, P. (2003). The water-filled versus air-filled status of vessels cut open in air: the 'Scholander assumption'revisited. *Plant, Cell & Environment*, *26*(4), 613-621.

Tyree, M. T., & Yang, S. (1990). Water-storage capacity of Thuja, Tsuga and Acer stems measured by dehydration isotherms. *Planta*, *182*(3), 420-426.

Van Mantgem, P. J., & Stephenson, N. L. (2007). Apparent climatically induced increase of tree mortality rates in a temperate forest. *Ecology Letters*, *10*(10), 909-916.

Venturas, M. D., Sperry, J. S., & Hacke, U. G. (2017). Plant xylem hydraulics: what we understand, current research, and future challenges. *Journal of Integrative Plant Biology*, *59*(6), 356-389.

Vergeynst, L. L., Dierick, M., Bogaerts, J. A., Cnudde, V., & Steppe, K. (2015). Cavitation: a blessing in disguise? New method to establish vulnerability curves and assess hydraulic capacitance of woody tissues. *Tree Physiology*, *35*(4), 400-409.

Vile, D., Shipley, B., & Garnier, E. (2006). A structural equation model to integrate changes in functional strategies during old-field succession. *Ecology*, *87*(2), 504-517.

Waring, R. H., Whitehead, D., & Jarvis, P. G. (1979). The contribution of stored water to transpiration in Scots pine. *Plant, Cell & Environment*, *2*(4), 309-317.

Wheeler, J. K., Sperry, J. S., Hacke, U. G., & Hoang, N. (2005). Inter-vessel pitting and cavitation in woody Rosaceae and other vesselled plants: a basis for a safety versus efficiency trade-off in xylem transport. *Plant, Cell & Environment*, *28*(6), 800-812.

Wolfe, B. T., & Kursar, T. A. (2015). Diverse patterns of stored water use among saplings in seasonally dry tropical forests. *Oecologia*, *179*(4), 925-936

Zhang, Y. J., Meinzer, F. C., QI, J. H., Goldstein, G., & CAO, K. F. (2013). Midday stomatal conductance is more related to stem rather than leaf water status in subtropical deciduous and evergreen broadleaf trees. *Plant, Cell & Environment*, *36*(1), 149-158.

Appendix 1. The species, biome type, variables measured, and citation for all studies used in the meta-analysis. The variables measured were: ρ_w (g/cm^3; sapwood density), P50 (MPa; water potential at fifty percent loss of conductivity), π_o (MPa; sapwood osmotic potential at full turgor), ε (MPa; total sapwood bulk elastic modulus), θ_s (m^3 m^{-3} ; sapwood saturated water content), C_{ft} (kg m^3 Mpa$^{-1)}$; sapwood capacitance at full turgor), Ψ_{tlp} (MPa; sapwood water potential at turgor loss point), and RWC_{tlp} (total sapwood relative water content at turgor loss point).

Species	Biome	ρ_w	P50	π_o	ε	θ_s	C_{ft}	Ψ_{tlp}	RWC_{tlp}	Citation
Abies grandis	BOR	*	*				*			McCulloh et al. 2014
Acacia doratoxylon	TDC	*		*	*	*	*	*	*	Richards et al. 2014
Acacia floribunda	TDC	*		*	*	*	*	*	*	Richards et al. 2014
Acacia greggii	MED	*		*	*	*	*	*	*	Pratt, unpublished
Acacia havilandiorum	TDC	*		*	*	*	*	*	*	Richards et al. 2014
Acacia suaveolens	TDC	*		*	*	*	*	*	*	Richards et al. 2014
Acalypha diversifolia	TRF	*		*	*	*	*	*	*	Bucior, unpublished
Acer campestre	TDC	*	*	*	*	*		*	*	Rosner et al. 2018
Adansonia rubrostipa	SAV	*		*		*		*		Chapotin et al. 2006
Adansonia za	SAV			*		*		*		Chapotin et al. 2006
Adenostoma fasciculatum	MED	*		*	*	*	*	*	*	Pratt, unpublished
Adenostoma sparsifolium	MED	*		*	*	*	*	*	*	Pratt, unpublished
Ambrosia Salsola	MED	*	*	*	*	*	*	*	*	Pratt, unpublished
Ampelopsis glandulosa	MED			*	*	*	*	*	*	Pratt, unpublished
Anacardium excelsum	TRF	*	*	*	*	*	*	*	*	Johnson et al. 2013
Anisoptera laevis	SAV	*		*	*	*	*	*	*	Siddiq et al. 2019
Annona spraguei	TRF	*	*	*	*	*	*	*	*	De Guzman et al. 2017
Anogeissus acuminata	SAV	*		*	*	*	*	*	*	Siddiq et al. 2019
Apeiba membranacea	TFR	*	*	*	*	*	*	*	*	De Guzman, submitted
Arctostaphylos glauca	MED	*		*	*	*	*	*	*	Pratt, unpublished
Astronium graveolens	TRF	*	*	*	*	*	*	*	*	De Guzman, submitted
Astrotricha floccose	TDC	*		*	*	*	*	*	*	Richards et al. 2014

Baccharis uncinella	SAV	*		*	*	*	*	*	*	Rosado, unpublished
Balfourodendron riedelianum	TRF	*		*	*		*	*	*	Carrasco et al. 2014
Bernardia myricifolia	MED			*	*	*	*	*	*	Pratt, unpublished
Bertya cunninghamii	TDC	*		*	*	*	*	*	*	Richards et al. 2014
Betula alnoides	BOR	*					*			Zhang et al. 2013
Betula occidentalis	BOR	*					*			Fu et al. 2019
Beyeria opaca	TDC	*		*	*	*	*	*	*	Richards et al. 2014
Blepharocalyx salicifolius	SAV	*		*	*	*	*	*	*	Scholz et al. 2007
Bocoa prouacensis	TRF	*	*	*	*	*	*	*	*	Santiago et al. 2018
Boronia ledifolia	TDC	*		*	*	*	*	*	*	Richards et al. 2014
Brachychiton populneus	TDC	*		*	*	*	*	*	*	Richards et al. 2014
Brickellia californica	MED			*	*	*	*	*	*	Pratt, Unpublished
Brosimum utile	TRF	*	*	*	*	*	*	*	*	De Guzman, submitted
Byrsonima crassifolia	SAV	*		*	*	*	*	*	*	Scholz et al. 2007
Byrsonima sericea	SAV	*		*	*			*		Rosado et al. 2010
Cabralea canjerana	TRF	*		*	*		*	*	*	Carrasco et al. 2014
Calophyllum longifolium	TRF	*		*	*	*	*	*	*	Bucior, unpublished
Caryocar brasiliense	SAV	*		*	*	*	*	*	*	Scholz et al. 2007
Cassinia laevis	TDC	*		*	*	*	*	*	*	Richards et al. 2014
Cassipourea elliptica	TRF	*		*	*	*	*	*	*	Bucior, unpublished
Ceanothus crassifolius	MED	*		*	*	*	*	*	*	Pratt et al. 2007
Ceanothus cuneatus	MED	*		*	*	*	*	*	*	Pratt et al. 2007
Ceanothus spinosus	MED			*	*	*	*	*	*	Pratt et al. 2007
Cedrela fissilis	TRF	*		*	*	*	*	*	*	Carrasco et al. 2014
Cieba speciosa	TRF	*		*	*		*	*	*	Carrasco et al. 2014

Cercocarpus Betuloides	MED	*		*	*	*	*	*	*	Pratt, unpublished
Cercocarpus ledifolius	TDC	*					*			Fu et al. 2019
Chionolaena capitata	SAV			*	*	*	*	*	*	Rosado, unpublished
Chrysophyllum gonocarpum	TRF	*		*	*		*	*	*	Carrasco et al. 2014
Citrus sinensis	MED	*		*	*			*	*	Bucior, unpublished
Clethra brammeriana	BOR	*					*			Zhang et al. 2013
Combretum fruticosum	TRF	*	*	*	*	*	*	*	*	De Guzman et al. 2017
Cordia aliodora	TRF	*	*	*	*	*	*	*	*	De Guzman et al. 2017
Cordia trichotoma	TRF			*	*		*	*	*	Carrasco et al. 2014
Cupressus arizonica	TDC			*	*	*	*	*	*	Bucior, unpublished
Dalbergia fusca	SAV	*		*	*	*	*	*	*	Siddiq et al. 2019
Dalbergia odorifera	SAV	*		*	*	*	*	*	*	Siddiq et al. 2019
Dicorynia guianensis	TRF	*	*	*	*	*	*	*	*	Santiago et al. 2018
Dipterocarpus alatus	SAV	*		*	*	*	*	*	*	Siddiq et al. 2019
Dipterocarpus tuberculatus	SAV	*		*	*	*	*	*	*	Siddiq et al. 2019
Dodonaea viscosa	TDC	*		*	*	*	*	*	*	Richards et al. 2014
Doliocarpus dentatus	TRF	*	*	*	*	*	*	*	*	De Guzman et al. 2017
Doliocarpus multiflorus	TRF	*	*	*	*	*	*	*	*	De Guzman, submitted
Dussia munda	TRF	*	*	*	*	*	*	*	*	De Guzman, submitted
Encelia actoni	MED	*		*	*	*	*	*	*	Pivovaroff et al. 2016
Encelia californica	MED	*		*	*	*	*	*	*	Pratt, unpublished
Eperua falcata	TRF	*	*	*	*	*	*	*	*	Santiago et al. 2018
Epeura grandiflora	TRF	*	*	*	*	*	*	*	*	Santiago et al. 2018
Ephedra californiaca	MED	*	*	*	*	*	*	*	*	Pivovaroff et al. 2016
Eremophila glabra	TDC	*		*	*	*	*	*	*	Richards et al. 2014

Eremophila longifolia	TDC	*		*	*	*	*	*	*	Richards et al. 2014
Ericameria linearifolia	MED	*	*	*	*	*	*	*	*	Pivovaroff et al. 2016
Ericameria parishii	MED			*	*	*	*	*	*	Pratt, unpublished
Eriogonum cinereum	MED			*	*	*	*	*	*	Pratt, unpublished
Eriostemon australaisus	TDC	*		*	*	*	*	*	*	Richards et al. 2014
Eythroxylum ovalifolium	SAV	*		*	*			*		Rosado et al. 2010
Eschweilera sagotiana	TRF	*	*	*	*	*	*	*	*	Santiago et al. 2018
Eucalyptus socialis	TDC	*		*	*	*	*	*	*	Richards et al. 2014
Eugenia umbeliflora	SAV	*		*	*			*		Rosado et al. 2010
Fagus sylvatica	TDC	*					*			Jupa et al. 2016
Ficus insipida	TRF	*	*	*	*		*	*	*	Meinzer et al. 2003
Fraxinus dipetala	MED	*		*	*	*	*	*	*	Pratt, unpublished
Geijera parviflora	TDC	*		*	*	*	*	*	*	Richards et al. 2014
Gustavia Superba	TRF	*		*	*	*	*	*	*	Bucior, unpublished
Hakea dactloides	TDC	*		*	*	*	*	*	*	Richards et al. 2014
Hakea tephrosperma	TDC	*		*	*	*	*	*	*	Richards et al. 2014
Heteromeles arbutifolia	MED			*	*	*	*	*	*	Zhang et al. 2013
Holocalyx balansae	TRF	*		*	*		*	*	*	Carrasco et al. 2014
Hopea hainanensis	SAV	*		*	*	*	*	*	*	Siddiq et al. 2019
Ilex aquifolium	TDC	*		*	*	*	*	*	*	Bucior, unpublished
Illicium macranthum	BOR	*					*			Zhang et al. 2013
Jacaranda copaia	TRF	*	*	*	*	*	*	*	*	Santiago et al. 2018
Juniperus californica	MED	*	*	*	*	*	*	*	*	Pivovaroff et al. 2016
Keckiella ternata	MED			*	*	*	*	*	*	Pratt, unpublished
Kielmeyera coriacea	SAV	*		*	*	*	*	*	*	Scholz et al. 2007

Lambertia formosa	TDC	*		*	*	*	*	*	*	Richards et al. 2014
Larix decidua	TDC	*	*	*	*	*		*	*	Rosner et al. 2019
Lasiopetalum ferrugineum	TDC	*		*	*	*	*	*	*	Richards et al. 2014
Lecythis persistens	TRF	*	*	*	*	*	*	*	*	Santiago et al. 2018
Leptospermum trinevium	TDC	*		*	*	*	*	*	*	Richards et al. 2014
Licania alba	TRF	*	*	*	*	*	*	*	*	Santiago et al. 2018
Liciana heteromorpha	TRF	*	*	*	*	*	*	*	*	Santiago et al. 2018
Lomatia silaifolia	TDC	*		*	*	*	*	*	*	Richards et al. 2014
Lonchocarpus muehlbergianus	TRF	*		*	*		*	*	*	Carrasco et al. 2014
Luehea seemannii	TRF	*	*	*	*	*	*	*	*	Pivovaroff et al. 2016
Lyonia ovalifolia	BOR	*					*			Zhang et al. 2013
Malosma laurina	ME	*	*							Unpublished, Pratt
Manglietia insignis	BOR	*					*			Zhang et al. 2013
Manilkara bidentata	TRF	*	*	*	*	*	*	*	*	Pivovaroff et al. 2016
Manilkara subsericea	SAV	*		*	*			*		Rosado et al. 2010
Maripa panamensis	TRF	*	*	*	*	*	*	*	*	Pivovaroff et al. 2016
Maytensu obtusifolia	SAV	*		*	*			*		Rosado et al. 2010
Melaleuca uncinata	TDC	*		*	*	*	*	*	*	Richards et al. 2014
Mesua ferrea	SAV	*		*	*	*	*	*	*	Siddiq et al. 2019
Mikania leiostacya	TRF	*	*	*	*	*	*	*	*	De Guzman et al. 2017
Myrsine parvifolia	SAV	*		*	*			*		Rosado et al. 2010
Nectandra purpurea	TRF	*		*	*	*	*	*	*	Bucior, unpublished
Nicotiana glauca	BOR			*	*	*	*	*	*	Bucior, unpublished
Notholithocarpus jindongensis	BOR	*					*			McCulloh et al. 2014
Notholithocarpus densiflorus	TDC			*	*	*	*	*	*	Bucior, unpublished

Notholithocarpus hypoviridis	BOR	*					*			McCulloh et al. 2014
Ochroma pyramidale	TRF	*	*	*	*	*	*	*	*	De Guzman, submitted
Ocotea diospyrifolia	TRF	*		*	*		*	*	*	Carrasco et al. 2014
Ocotea notata	SAV	*		*	*		*	*		Rosado et al. 2010
Olea europea	MED	*		*	*		*	*	*	Lopez et al. 2014
Olearia pimeleoides	TDC	*		*	*	*		*	*	Richards et al. 2014
Palicourea guianensis	TRF	*		*	*	*	*	*	*	Bucior, unpublished
Parapiptadenia rigida	TRF	*		*	*		*	*	*	Carrasco et al. 2014
Parashorea chinensis	SAV	*		*	*	*	*	*	*	Siddiq et al. 2019
Persoonia levis	TDC	*		*	*	*	*	*	*	Richards et al. 2014
Persoonia linearis	TDC	*		*	*	*	*	*	*	Richards et al. 2014
Philotheca difformis	TDC	*		*	*	*	*	*	*	Richards et al. 2014
Phoebe puwenensis	SAV	*		*	*	*	*	*	*	Siddiq et al. 2019
Phoenix reclinata	TRF	*	*	*	*	*	*	*	*	De Guzman, submitted
Phyllota phylicoides	TDC	*		*	*	*	*	*	*	Richards et al. 2014
Piecea abies	BOR	*		*	*	*	*	*	*	Bucior, unpublished
Pinus contorta	BOR	*					*			Running, 1979
Pinus ponderosa	BOR	*	*	*	*		*	*	*	Barnard et al. 2011
Pinus sylvestris	TDC	*		*	*	*	*	*	*	Waring et al. 1979
Pittosporum tobira	TDC			*	*	*	*	*	*	De Guzman, submitted
Pleroma hospita	SAV			*	*	*	*	*	*	Rosado, unpublished
Populus canescens	TDC	*	*	*	*	*		*	*	Rosner et al. 2019
Populus tremula	TDC	*	*	*	*	*		*	*	Rosner et al. 2019
Populus yunnanensis	BOR	*					*			Zhang et al. 2013
Poulsenia armata	TRF	*		*	*	*	*	*	*	Bucior, unpublished

Pourouma bicolor	TRF	*		*	*	*	*	*	*	Bucior, unpublished
Pradosia cochlearia	TRF	*	*	*	*	*	*	*	*	Santiago et al. 2018
Protium icicariba	SAV	*		*	*			*	*	Rosado et al. 2010
Protium panamense	TRF	*		*	*	*	*	*	*	Bucior, unpublished
Prunus dulcis	MED	*		*	*			*	*	López-Bernal et al. 2014
Prunus fasciculata	MED	*	*	*	*	*	*	*	*	Pivovaroff et al. 2016
Pseudobombax septenatum	TRF	*	*				*			Machado et al. 1994
Pseudotsuga menziesii	BOR	*	*	*	*		*	*	*	Barnard et al. 2011
Psorothamnus arborescens	MED	*	*	*	*	*	*	*	*	Pivovaroff et al. 2016
Pterocarpus indicus	SAV	*		*	*	*	*	*	*	Siddiq et al. 2019
Pultenaea flexilis	TDC	*		*	*	*	*	*	*	Richards et al. 2014
Purshia tridentata	MED	*	*	*	*	*	*	*	*	Pivovaroff et al. 2016
Qualea parviflora	SAV	*		*	*	*	*	*	*	Scholz et al. 2007
Quercus alba	TDC	*		*	*	*	*	*	*	Bucior, unpublished
Quercus berberidifolia	MED			*	*	*	*	*	*	Pratt, unpublished
Quercus cornelius	MED			*	*	*	*	*	*	Pratt, unpublished
Quercus cornelius-mulleri	MED	*	*	*	*	*	*	*	*	Pivovaroff et al. 2016
Quercus garryana	BOR	*					*			Fu et al. 2019
Quercus john-tuckeri	MED	*	*	*	*	*	*	*	*	Pivovaroff et al. 2016
Quercus robur	TDC	*					*			Jupa et al. 2016
Quercus wislizeni	MED			*	*	*	*	*	*	Pratt, unpublished
Rhamnus ilicifolia	MED			*	*	*	*	*	*	Pratt, unpublished
Rhus ovata	MED	*	*	*	*	*	*	*	*	Pratt, unpublished
Rhus trilobata	MED			*	*	*	*	*	*	Pratt, unpublished
Ribes malvaceum	MED			*	*	*	*	*	*	Pratt, unpublished

Ribes speciosum	MED	*		*	*	*	*	*	*	Pratt, unpublished
Robinia pseudoacacia	TDC	*					*			Jupa et al. 2016
Sabal palmetto	TRF			*	*		*	*	*	Holbrook et al. 1992
Salix scouleriana	BOR	*					*			Fu et al. 2019
Sambucus mexicana	MED	*		*	*	*	*	*	*	Pratt, unpublished
Schefflera macrocarpa	SAV	*		*	*	*	*	*	*	Scholz et al. 2007
Schefflera morototoni	TRF	*	*	*	*		*	*	*	Meinzer et al. 2003
Schima norohae	BOR	*					*			Zhang et al. 2013
Sclerolobium paniculatum	SAV			*	*	*	*	*	*	Scholz et al. 2007
Scutellaria mexicana	MED	*	*	*	*	*	*	*	*	Pivovaroff et al. 2016
Senegalia greggi	MED	*	*	*	*	*	*	*	*	Pivovaroff et al. 2016
Senna artemisioides	TDC	*		*	*	*	*	*	*	Richards et al. 2014
Sequoia sempervirens	TDC	*		*	*	*	*	*	*	Bucior, unpublished
Serjania mexicana	TRF	*	*	*	*	*	*	*	*	De Guzman et al. 2017
Sextonia rubra	TRF	*	*	*	*	*	*	*	*	Santiago et al. 2018
Shorea assamica	SAV	*		*	*	*	*	*	*	Siddiq et al. 2019
Sorbus torminalis	TDC	*	*	*	*	*		*	*	Rosner et al. 2019
Stewartia pteropetiolata	BOR	*					*			Zhang et al. 2013
Swietenia macrophylla	SAV	*		*	*	*	*	*	*	Siddiq et al. 2019
Symphonia globulifera	TRF	*	*	*	*	*	*	*	*	Santiago et al. 2018
Symplocos sumuntia	BOR	*					*			Zhang et al. 2013
Syncarpia glomulifera	TDC	*		*	*	*	*	*	*	Richards et al. 2014
Synoum glandulosum	TDC	*		*	*	*	*	*	*	Richards et al. 2014
Tachigali melinonii	TRF	*	*	*	*	*	*	*	*	Santiago et al. 2018
Tachigali versicolor	TRF	*	*	*	*		*	*	*	De Guzman, submitted

Tapiria guianensis	TRF	*	*	*	*		*	*	*	De Guzman, submitted
Ternstroemia brasiliensis	SAV	*		*	*			*		Rosado et al. 2010
Ternstroemia gymnanthera	BOR	*		*	*	*	*	*	*	Zhang et al. 2013
Thamnosma montana	MED	*	*	*	*	*	*	*	*	Pivovaroff et al. 2016
Thuja occidentalis	BOR	*					*			Tyree et al. 2010
Thuja plicata	BOR	*	*				*			McCulloh et al. 2014
Tilia cordata	TDC	*					*			Jupa et al. 2016
Tontelea ovalifolia	TRF	*	*	*	*	*	*	*	*	De Guzman, submitted
Trattinnickia aspera	TRF	*	*	*	*		*	*	*	De Guzman, submitted
Trichanthera gigantea	TRF	*	*	*	*	*	*	*	*	De Guzman, submitted
Tsuga canadensis	BOR	*					*			Tyree et al. 2010
Vaccinium delavayi	BOR	*					*			Zhang et al. 2013
Varica mangachapoi	SAV	*		*	*	*	*	*	*	Siddiq et al. 2019
Virola elongata	TRF	*	*	*	*	*	*	*	*	De Guzman, submitted
Vitis vinifera	TDC	*			*			*		Vergeynst et al. 2014
Vochysia ferruginea	TRF	*	*	*	*		*	*	*	De Guzman, submitted
Vochysia thyrsoidea	SAV	*		*	*	*	*	*	*	Scholz et al. 2007
Vouacapoua americana	TRF	*	*	*	*	*	*	*	*	Santiago et al. 2018
Ziziphus parryi	MED			*	*	*	*	*	*	Pivovaroff et al. 2016